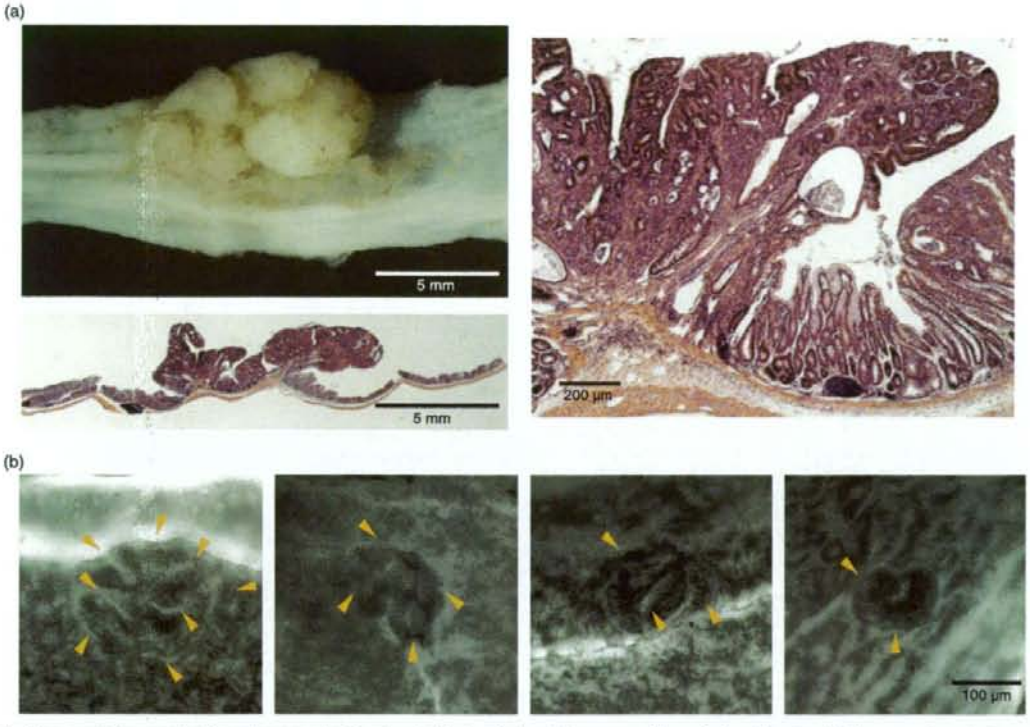

Fig. 2. Representative neoplastic and preneoplastic colorectal lesions induced by azoxymethane in *Snark*$^{+/-}$ mice. (a) Macroscopic and microscopic views of a tubular adenoma that developed in a *Snark*$^{+/-}$ mouse. The microscopic views were acquired using hematoxylin–eosin staining. Original magnification: left bottom, ×4; right, ×100. (b) Representative features of aberrant crypt foci (ACF). ACF were detected using methylene blue staining. The arrowheads indicate the luminal openings of the crypts. Original magnification: ×40.

Table 3. Age, bodyweight, and aberrant crypt foci (ACF) induced by short-term azoxymethane (AOM) treatment in *Snark*$^{+/+}$, *Snark*$^{+/-}$, and *Snark*$^{-/-}$ mice

Genotype	+/+	+/−	+/+	+/−	−/−
Number of animals	5	5	5	6	5
Age (months)†	6	6	2	2	2
AOM administration (weeks)	2	2	4	4	4
Bodyweight (g)†	34.49 ± 1.22	39.72 ± 1.65§	29.51 ± 0.45	28.79 ± 0.80	26.90 ± 1.09
Incidence of ACF‡	2/5	5/5	4/5	6/6	5/5
Number of foci/colon	2.00 ± 1.00	6.60 ± 1.69§	0.80 ± 0.20	1.50 ± 0.20¶	4.00 ± 1.26§
Mean number of aberrant crypts/focus	1.00 ± 0	1.00 ± 0	1.20 ± 0.37	1.00 ± 0	1.22 ± 0.15

†Values at the time of dissection. ‡Number of mice with aberrant crypt foci/total mice. §¶Significantly different from the corresponding values in *Snark*$^{+/+}$ mice at levels of $P < 0.01$ and $P < 0.05$, respectively.

in the *Snark*$^{+/-}$ mice (1.50 ± 0.20) than in the *Snark*$^{+/+}$ mice (0.80 ± 0.20), and the number was much higher in the *Snark*$^{-/-}$ mice (4.00 ± 1.26).

Discussion

To clarify the physiological roles of SNARK, we established *Snark*-deficient mice. *Snark*$^{+/-}$ mice developed normally and did not exhibit any obvious abnormalities. No significant differences in bodyweight were observed between *Snark*$^{+/-}$ and *Snark*$^{+/+}$ mice at the time of weaning. However, *Snark*$^{+/-}$ mice fed ordinary mouse chow exhibited mature-onset obesity at 4 months of age and thereafter. Although the food intake was not increased, oxygen consumption was decreased in the *Snark*$^{+/-}$ mice (K. Tsuchihara *et al.*, manuscript in preparation, 2008). Thus, we assume that lower energy consumption caused the obesity of *Snark*$^{+/-}$ mice. Mature *Snark*$^{+/-}$ mice exhibited significant fat deposition accompanied with metabolic disorders, like glucose intolerance and increased serum triglyceride level. Interestingly, the serum free fatty acid concentration was significantly reduced in *Snark*$^{+/-}$ mice. Together, these findings suggest that fat synthesis and deposition were enhanced. Meanwhile, fat utilization

doi: 10.1111/j.1349-7006.2008.00734.x

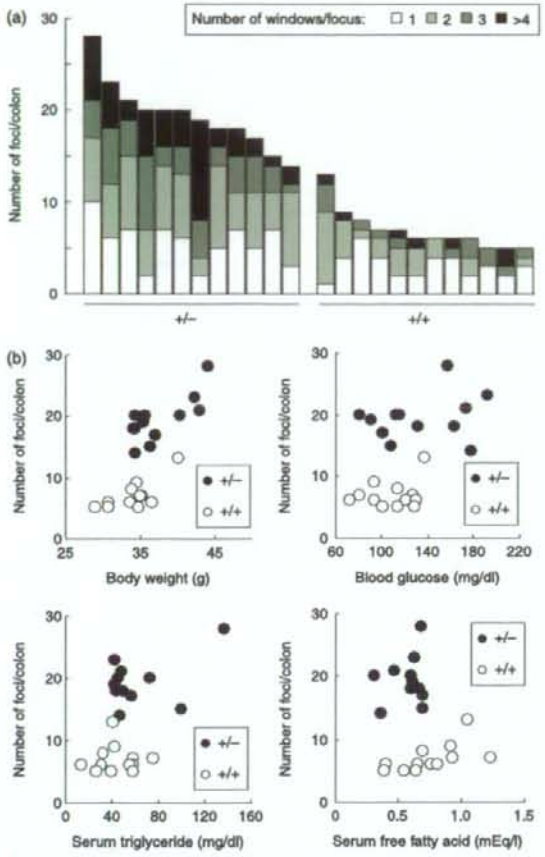

Fig. 3. Distribution of aberrant crypt focus (ACF) size, and correlation between ACF and obesity in *Snark*$^{+/-}$ and *Snark*$^{+/+}$ mice. (a) Total number and size distribution of ACF in each mouse. (b) Correlation between ACF numbers and bodyweight or metabolic parameters. Significant correlations between bodyweight and ACF number were observed in both *Snark*$^{+/-}$ and *Snark*$^{+/+}$ mice.

was impaired in *Snark*$^{+/-}$ mice (K. Tsuchihara *et al.*, manuscript in preparation, 2008). AOM-treated mice showed similar findings to those observed in AOM-untreated mice (Table 2), suggesting that AOM treatment did not affect the impairment of metabolic regulation that is characteristic of *Snark*$^{+/-}$ mice.

Aberrant crypt foci are regarded as preneoplastic lesions in rodent models and humans.[19–25] Although the C57BL/6 strain is known to be resistant to the induction of colon tumors by AOM,[26] at least one ACF was detected in all of the mice in the long-term experiment (Table 2). The high AOM dose and the relatively long experimental period might have contributed to the increased susceptibility to ACF formation seen in wild-type mice. However, the number of ACF was significantly higher in the *Snark*$^{+/-}$ mice compared with the *Snark*$^{+/+}$ mice. The multiplicity of each ACF was also different. Moreover, the incidence of tumorigenesis was significantly higher in the *Snark*$^{+/-}$ mice (Table 2). These results strongly suggest that the hemiallelic loss of *Snark* contributed to an increase in the frequency of carcinogen-induced neoplastic and preneoplastic lesions. As no spontaneous tumors were detected in age-matched or older untreated mice, the colorectal tumorigenesis observed in this experiment might have depended on the AOM treatment. The short-term experiment revealed that the loss of *Snark* expression affected the incidence of AOM-induced carcinogenesis initiation (Table 3). The profile of the proliferating cell population was not different between the *Snark*$^{+/-}$ and *Snark*$^{+/+}$ mice (Table 2). It also suggests that the *Snark* deficiency participated in tumor formation but not in cell proliferation *in vivo*.

A significant correlation between the number of ACF and bodyweight was observed in both *Snark*$^{+/-}$ and *Snark*$^{+/+}$ mice. The dosage of AOM in the *Snark*$^{+/-}$ mice was 10% higher than that of the *Snark*$^{+/+}$ mice due to the bodyweight gain. According to the previous report, this difference is negligible on ACF formation.[27] These results suggest the obesity-dependent contribution of Snark deficiency to the susceptibility to carcinogen-induced preneoplastic lesions (Fig. 3b).

Meanwhile, plots of bodyweight versus ACF number showed that the ranges of ACF numbers were clearly different between *Snark*$^{+/-}$ and *Snark*$^{+/+}$ mice. The number of ACF was larger in the *Snark*$^{+/-}$ mice than in the *Snark*$^{+/+}$ mice when mice with similar bodyweights were compared, suggesting that *Snark* deficiency may contribute to ACF formation in a manner that is independent of obesity. To clarify this issue, preobese 4-week-old *Snark*$^{+/-}$, *Snark*$^{+/+}$, and surviving *Snark*$^{-/-}$ mice were treated with AOM. An increased number of ACF in *Snark*-deficient mice may support an obesity-independent function of Snark in the suppression of tumor formation.

The precise mechanisms responsible for the suppression of ACF formation by Snark remain to be elucidated. We plan to investigate the direct effect of Snark on the maintenance of genome integrity and the regulation of cell proliferation. How and which metabolic disorders are responsible for enhancing tumor susceptibility may also be an interesting line of study. We expect that *Snark*-deficient mice may be useful as a new rodent model for investigating the relationships between tumorigenesis and metabolic disorders.

Acknowledgments

This work was supported by the Japanese Ministry of Health, Labour, and Welfare for the Third-Term Comprehensive 10-Year Strategy for Cancer Control, and Grants-in-Aid for Cancer Research from the Japanese Ministry of Health, Labour, and Welfare and the Ministry of Education, Science, Sports, and Culture.

References

1 Hardie DG, Hawley SA, Scott JW. AMP-activated protein kinase–development of the energy sensor concept. *J Physiol* 2006; **574**: 7–15.
2 Kahn BB, Alquier T, Carling D, Hardie DG. AMP-activated protein kinase: ancient energy gauge provides clues to modern understanding of metabolism. *Cell Metab* 2005; **1**: 15–25.
3 Lizcano JM, Goransson O, Toth R *et al.* LKB1 is a master kinase that activates 13 kinases of the AMPK subfamily, including MARK/PAR-1. *EMBO J* 2004; **23**: 833–43.
4 Manning G, Whyte DB, Martinez R, Hunter T, Sudarsanam S. The protein kinase complement of the human genome. *Science* 2002; **298**: 1912–34.
5 Lefebvre DL, Bai Y, Shahmolky N *et al.* Identification and characterization of a novel sucrose-non-fermenting protein kinase/AMP-activated protein kinase-related protein kinase, SNARK. *Biochem J* 2001; **355**: 297–305.
6 Lefebvre DL, Rosen CF. Regulation of SNARK activity in response to cellular stresses. *Biochim Biophys Acta* 2005; **1724**: 71–85.
7 Suzuki A, Kusakai G, Kishimoto A, Minegichi Y, Ogura T, Esumi H. Induction of cell–cell detachment during glucose starvation through F-actin conversion by SNARK, the fourth member of the AMP-activated protein kinase catalytic subunit family. *Biochem Biophys Res Commun* 2003; **311**: 156–61.

8 Cobb S, Wood T, Tessarollo L *et al.* Deletion of functional gastrin gene markedly increases colon carcinogenesis in response to azoxymethane in mice. *Gastroenterology* 2002; **123**: 516–30.
9 Cowey S, Hardy RW. The metabolic syndrome: A high-risk state for cancer? *Am J Pathol* 2006; **169**: 1505–22.
10 Cowey SL, Quast M, Belalcazar LM *et al.* Abdominal obesity, insulin resistance, and colon carcinogenesis are increased in mutant mice lacking gastrin gene expression. *Cancer* 2005; **103**: 2643–53.
11 Frezza EE, Wachtel MS, Chiriva-Internati M. Influence of obesity on the risk of developing colon cancer. *Gut* 2006; **55**: 285–91.
12 Hirose Y, Hata K, Kuno T *et al.* Enhancement of development of azoxymethane-induced colonic premalignant lesions in C57BL/KsJ-db/db mice. *Carcinogenesis* 2004; **25**: 821–5.
13 Niho N, Mutoh M, Komiya M, Ohta T, Sugimura T, Wakabayashi K. Improvement of hyperlipidemia by indomethacin in Min mice. *Int J Cancer* 2007; **121**: 1665–9.
14 Niho N, Mutoh M, Takahashi M, Tsutsumi K, Sugimura T, Wakabayashi K. Concurrent suppression of hyperlipidemia and intestinal polyp formation by NO-1886, increasing lipoprotein lipase activity in Min mice. *Proc Natl Acad Sci USA* 2005; **102**: 2970–4.
15 Niho N, Takahashi M, Kitamura T *et al.* Concomitant suppression of hyperlipidemia and intestinal polyp formation in Apc-deficient mice by peroxisome proliferator-activated receptor ligands. *Cancer Res* 2003; **63**: 6090–5.
16 Niho N, Takahashi M, Shoji Y *et al.* Dose-dependent suppression of hyperlipidemia and intestinal polyp formation in Min mice by pioglitazone, a PPARγ ligand. *Cancer Sci* 2003; **94**: 960–4.
17 Weber RV, Stein DE, Scholes J, Kral JG. Obesity potentiates AOM-induced colon cancer. *Dig Dis Sci* 2000; **45**: 890–5.
18 Krutovskikh VA, Turusov VS. Tumours of the intestines. In: Turusov VS, Mohr U, eds. *Pathology of Tumours in Laboratory Animals*, 2nd edn. Lyon: International Agency for Research on Cancer, 1994; 195–211.
19 Bird RP. Role of aberrant crypt foci in understanding the pathogenesis of colon cancer. *Cancer Lett* 1995; **93**: 55–71.
20 Hata K, Yamada Y, Kuno T *et al.* Tumor formation is correlated with expression of β-catenin-accumulated crypts in azoxymethane-induced colon carcinogenesis in mice. *Cancer Sci* 2004; **95**: 316–20.
21 Hurlstone DP, Cross SS. Role of aberrant crypt foci detected using high-magnification-chromoscopic colonoscopy in human colorectal carcinogenesis. *J Gastroenterol Hepatol* 2005; **20**: 173–81.
22 Nambiar PR, Nakanishi M, Gupta R *et al.* Genetic signatures of high- and low-risk aberrant crypt foci in a mouse model of sporadic colon cancer. *Cancer Res* 2004; **64**: 6394–401.
23 Pretlow TP, Pretlow TG. Mutant KRAS in aberrant crypt foci (ACF): initiation of colorectal cancer? *Biochim Biophys Acta* 2005; **1756**: 83–96.
24 Takahashi M, Minamoto T, Yamashita N, Kato T, Yazawa K, Esumi H. Effect of docosahexaenoic acid on azoxymethane-induced colon carcinogenesis in rats. *Cancer Lett* 1994; **83**: 177–84.
25 Yamashita N, Minamoto T, Onda M, Esumi H. Increased cell proliferation of azoxymethane-induced aberrant crypt foci of rat colon. *Jpn J Cancer Res* 1994; **85**: 692–8.
26 Suzuki R, Kohno H, Sugie S, Nakagama H, Tanaka T. Strain differences in the susceptibility to azoxymethane and dextran sodium sulfate-induced colon carcinogenesis in mice. *Carcinogenesis* 2006; **27**: 162–9.
27 McLellan EA, Bird RP. Aberrant crypts: potential preneoplastic lesions in the murine colon. *Cancer Res* 1988; **48**: 6187–92.

doi: 10.1111/j.1349-7006.2008.00734.x

Biochemical and Biophysical Research Communications 380 (2009) 171–176

Contents lists available at ScienceDirect

Biochemical and Biophysical Research Communications

journal homepage: www.elsevier.com/locate/ybbrc

Inhibitors of insulin-like growth factor-1 receptor tyrosine kinase are preferentially cytotoxic to nutrient-deprived pancreatic cancer cells

Isao Momose *, Setsuko Kunimoto, Michiyo Osono, Daishiro Ikeda

Numazu Bio-Medical Research Institute, Microbial Chemistry Research Center, 18-24 Miyamoto, Numazu, Shizuoka 410-0301, Japan

ARTICLE INFO

Article history:
Received 8 January 2009
Available online 21 January 2009

Keywords:
IGF-1R
IGF-1R kinase inhibitor
AG1024
Nutrient starvation
Pancreatic cancer

ABSTRACT

Chronic deprivation of nutrients is rare in normal tissues, however large areas of tumor are nutrient-starved and hypoxic due to a disorganized vascular system. Some cancers show an inherent ability to tolerate severe growth conditions. Therefore, we screened chemical compounds to identify cytotoxic agents that function preferentially in nutrient-deprived conditions. We found that AG1024, a specific inhibitor of insulin-like growth factor-1 receptor tyrosine kinase (IGF-1R), showed preferential cytotoxicity to human pancreatic cancer cells in nutrient-deprived conditions relative to cells in nutrient-sufficient conditions. The cytotoxicity of I-OMe-AG538 (another specific inhibitor of IGF-1R kinase) was also enhanced in nutrient-deprived cells. In addition, AG1024 and I-OMe-AG538 potently inhibited IGF-1R activation to nutrient-deprived cells. In contrast, conventional chemotherapeutic drugs, as well as inhibitors of PDGFR and EGFR kinases, elicited weak cytotoxicity. These data indicate that nutrient-deprived human pancreatic cancer cells have increased sensitivity to inhibition of IGF-1R activation. IGF-1R inhibitors offer a promising strategy for anticancer therapeutic approaches that are oriented toward tumor microenvironment.

Patients diagnosed with pancreatic cancer, an aggressive disease with the lowest 5-year survival rates of all cancers, develop metastases rapidly and die within a short period of time after diagnosis [1,2]. Pancreatic cancer is largely resistant to almost all known chemotherapeutic agents, including 5-fluorouracil, paclitaxel and doxorubicin; surgery is the only current treatment modality that offers any prospect of potential cure. Clearly, there is a dire need for new therapeutic alternatives that improve clinical outcome for pancreatic cancer patients.

Tumor microenvironment exerts an important influence on cancer physiology. The disorganized vascular system in a tumor often results in large areas of tumor starved for nutrients and oxygen. Pancreatic cancers in particular, which are characterized as hypovascular tumors, show an inherent ability to tolerate severe growth conditions. Certain human pancreatic cancer cell lines, including PANC-1, AsPC-1, BxPC-3 and KP-3, exhibit marked environmental tolerance and can survive for prolonged periods of time in nutrient-deprived conditions. Because tolerance of these cancer cells to nutrient starvation has been associated with the activity of protein kinase B (PKB)/Akt [3], it has been hypothesized that agents that diminish such tolerance could function as anticancer agents [4–7].

Insulin-like growth factors-1 (IGF-1) and -2 (IGF-2) are involved in the pathophysiology of a wide range of human neoplasias due to the mitogenic and antiapoptotic properties mediated by their type 1 receptor (IGF-1R) [8]. IGF-1R is a tetrameric transmembrane receptor tyrosine kinase composed of two α and β subunits. The extracellular α subunit is responsible for ligand binding, whereas the β subunit consists of a transmembrane domain and an intracellular tyrosine kinase domain [9,10]. Ligand binding activates the intrinsic receptor tyrosine kinase, resulting in trans-β subunit autophosphorylation and stimulation of PI3K-AKT-TOR and RAF-MAPK signaling pathways. In addition to cell proliferation, activation of IGF-1R has been reported to stimulate cell survival, transformation, metastasis and angiogenesis [11]. Targeted inhibition of IGF-1R signaling has been shown to result in impressive anti-neoplastic activity in many *in vitro* and *in vivo* models of common human cancers. IGF-1R small interfering RNAs [12], anti-receptor antibodies [13,14], a IGF-1-like competitive peptide antagonist [15], a dominant-negative IGF-1R [16–18] and small-molecule IGF-1R tyrosine kinase inhibitors [19,20] have all been found to interfere with cell growth and proliferation. IGF-1R is therefore regarded as an attractive potential target in the development of new drugs to treat malignant tumors.

In this study, we screened chemical compounds to identify agents that preferentially reduce the survival of nutrient-deprived human pancreatic cancer PANC-1 cells. The screen identified IGF-1R inhibitors, which function as cytotoxic agents preferentially on human pancreatic cancer cells in nutrient-deprived conditions.

* Corresponding author. Fax: +81 55 922 6888.
E-mail address: imomose@bikaken.or.jp (I. Momose).

0006-291X/$ - see front matter © 2009 Elsevier Inc. All rights reserved.
doi:10.1016/j.bbrc.2009.01.065

Materials and methods

Materials. Antibodies used in Western blotting included anti-IGF-1Rβ (sc-713), anti-Erk 1 (sc-93) and anti-phospho-Erk (sc-7383) from Santa Cruz Biotechnology (Santa Cruz, CA); anti-α-tubulin (T5168) from Sigma–Aldrich (St. Louis, MO); and anti-Akt (#9272), anti-phospho-Akt (Ser 473) (#9271), anti-phospho-Akt (Thr 308) (#9275) and anti-phospho-IGF-1R (#3021) from Cell Signaling Technology (Denvers, MA). Recombinant human IGF-1 was from R&D Systems (Minneapolis, MN). AG1024, AG1296, AG1478 and I-OMe-AG538 were obtained from Calbiochem (Madison, WI). Doxorubicin hydrochloride, fluorouracil, paclitaxel and mitomycin C were from Sigma. The SCADS inhibitor kit I consisting of 79 chemical inhibitors with ~60 different targets was kindly provided by the Screening Committee on Anticancer Drugs (Japan).

Cells and culture. Human pancreatic cancer cell lines PANC-1, Capan-1, MIA Paca-2, BxPC-3 and PSN-1 were obtained from the American Type Culture Collection (Rockville, MD). Cells were grown at 37 °C with 5% CO_2 in Dulbecco's modified Eagle medium (DMEM; Nissui, Tokyo, Japan) supplemented with 10% fetal bovine serum (FBS; Tissue Culture Biologicals, Tulare, CA), 100,000 U/L penicillin G, and 100 mg/L streptomycin. Nutrient starvation was achieved by culturing the cells in nutrient-deprived medium (NDM) as previously described [3–7]. Briefly, the composition of the NDM was as follows: 265 mg/L $CaCl_2{\cdot}H_2O$, 400 mg/L KCl, 200 mg/L $MgSO_4{\cdot}7H_2O$, 6400 mg/L NaCl, 163 mg/L $NaH_2PO_4{\cdot}2H_2O$, 0.1 mg/L $Fe(NO_3)_3{\cdot}9H_2O$, 5 mg/L phenol red, 100,000 U/L penicillin G, 100 mg/L streptomycin, 25 mmol/L HEPES buffer (pH 7.4), and MEM vitamin solution (Invitorogen, Carlsbad, CA); the final pH was adjusted to 7.4 with 10% $NaHCO_3$.

Preferential cytotoxicity in nutrient-deprived conditions. PANC-1 cells (2.5×10^4 cells/well) in 96-well plates were cultured in DMEM for 24 h. The cells were washed with PBS and the medium was replaced with either fresh DMEM or NDM. Test samples were added to the well and cells were cultured for 24 h. Cytotoxicity was determined using the MTT assay [21].

Preparation of cell lysate and Western blotting. PANC-1 cells (5×10^5) in 35-mm dishes were incubated in DMEM for 24 h. The cells were washed with PBS and the medium was replaced with either fresh DMEM or NDM. AG1024 or I-OMe-AG538 was added to each dish and the cells were incubated for 1 h prior to stimulation with 50 ng/ml IGF-1 for 10 min. The cells were washed twice with ice-cold PBS containing 100 μm Na_3VO_4 and then lysed in a lysis buffer (20 mM *N*-2-hydroxyethylpiperazine-*N'*-2-ethanesulfonic acid, 150 mM NaCl, 1% Triton X-100, 10% glycerol, 1 mM EDTA, 50 mM NaF, 50 mM β-glycerolphosphate, 1 mM Na_3VO_4, pH 7.5, and 25 μg/ml each of antipain, leupeptin, and pepstatin). Equal amounts of protein extract were separated by SDS–polyacrylamide gel electrophoresis, transferred onto Immobilon polyvinylidene difluoride membranes (Millipore, Bedford, MA) and probed with anti-IGF-1R, anti-phospho-IGF-1R, anti-Akt, anti-phospho-Akt (Thr 308), anti-phospho-Akt (Ser 473), anti-Erk 1,

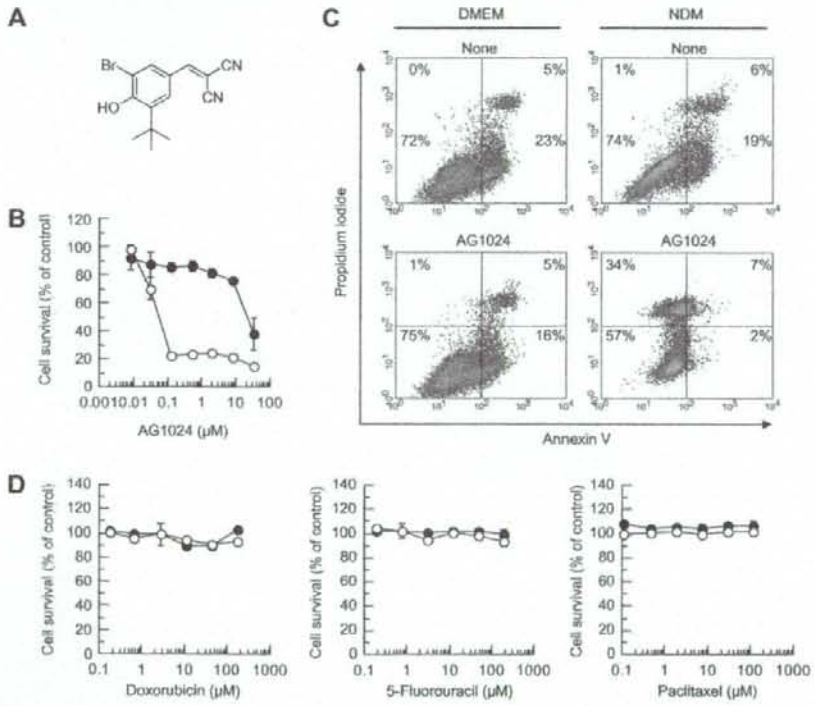

Fig. 1. Effect of AG1024 on survival of PANC-1 cells in nutrient-deprived conditions. (A) Structure of AG1024. (B) Effect of AG1024 on PANC-1 cell viability in normal medium, DMEM (●) and nutrient-deprived medium, NDM (○). PANC-1 cells incubated in DMEM for 24 h. The cells were then washed with PBS and the medium was replaced with either fresh DMEM or NDM. The indicated concentrations of AG1024 were added to each well and the cells were incubated for 24 h. Cell viability was determined using the MTT assay. (C) Flow cytometric analysis of AG1024-treated PANC-1 cells. PANC-1 cells were cultured with 0.3 μM AG1024 in DMEM or NDM for 12 h. The cells were stained with annexin V-FITC and propidium iodide according to instructions for the apoptosis detection kit and then analyzed using a flow cytometer. (D) Effect of conventional anticancer drugs on survival of PANC-1 cells in nutrient-deprived conditions. PANC-1 cells were incubated with indicated concentrations of doxorubicin, 5-fluorouracil and paclitaxel in DMEM (●) or NDM (○) for 24 h.

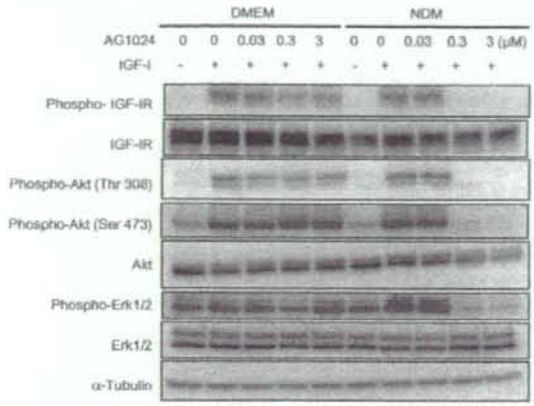

Fig. 2. Effect of AG1024 on IGF-1R activation. PANC-1 cells incubated in DMEM for 24 h were washed with PBS and the medium was replaced with either fresh DMEM or NDM. The cells were incubated with the indicated concentration of AG1024 for 1 h before stimulation with 50 ng/ml IGF-1 for 10 min. Cell lysates were resolved using SDS–PAGE and transferred to membranes for western blotting with specific antibodies.

anti-phospho-Erk, or anti-tubulin antibodies. Horseradish peroxidase-linked anti-rabbit IgG or anti-mouse IgG antibodies were used as secondary antibodies (GE Healthcare, Piscataway, NJ). The blots were developed using ECL reagent according to the manufacturer's instructions (GE healthcare).

Flow cytometric analysis. PANC-1 cells (5×10^5) in 60-mm dishes were incubated in DMEM for 24 h. The cells were washed with PBS and the medium was replaced with either fresh DMEM or NDM. AG1024 (0.3 μM) was then added and the cells were cultured for 12 h. The cells were incubated with annexin V-FITC and propidium iodide using an annexin V-FITC apoptosis detection kit (Biovision Research Products, Mountain View, CA) and analyzed using a flow cytometer (FACSCalibur; BD Biosciences, Franklin Lakes, NJ).

Statistical analysis. All data are representative of three independent experiments with similar results. The statistical data are expressed as mean ± SD using descriptive statistics.

Results

AG1024 is preferentially cytotoxic to human pancreatic cancer PANC-1 cells in nutrient-deprived conditions

To identify cytotoxic agents that function preferentially on nutrient-deprived cells, we tested the cytotoxic effects of small-molecule inhibitors in the SCADS inhibitors kit I. As shown in Table S1, a specific inhibitor of IGF-1R tyrosine kinase, termed AG1024, was found to be cytotoxic to PANC-1 cells in nutrient-deprived medium (NDM), but not in normal medium (DMEM). The structure of AG1024 [22], otherwise known as 2-(3-bromo-5-*t*-butyl-4-hydroxybenzylidene)malonitrile, is shown in Fig. 1A. To determine the dose–response relationship of AG1024 cytotoxicity, PANC-1

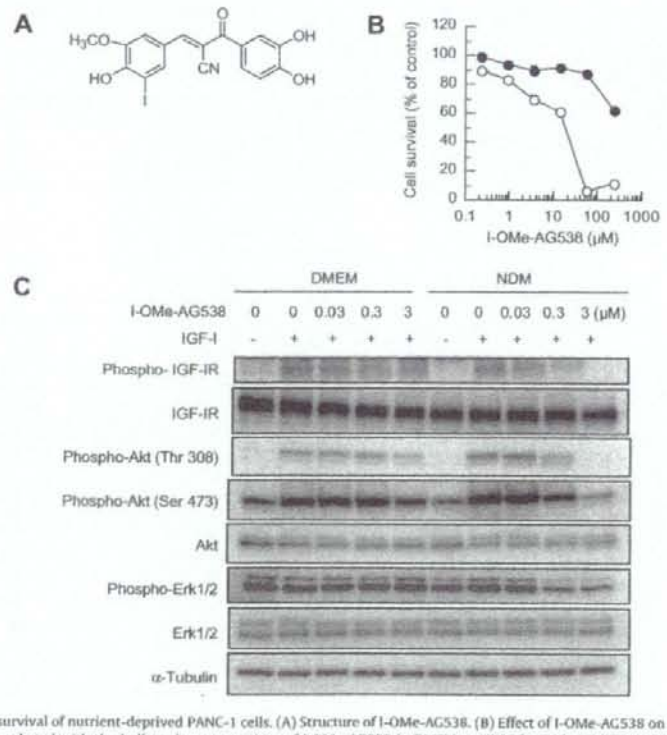

Fig. 3. Effect of I-OMe-AG538 on survival of nutrient-deprived PANC-1 cells. (A) Structure of I-OMe-AG538. (B) Effect of I-OMe-AG538 on PANC-1 cell viability in DMEM (●) or NDM (○). PANC-1 cells were incubated with the indicated concentrations of I-OMe-AG538 in DMEM or NDM for 24 h. (C) Effect of I-OMe-AG538 on IGF-1R activation. PANC-1 cells in DMEM or NDM were incubated with the indicated concentration of I-OMe-AG538 for 1 h before stimulation with 50 ng/ml IGF-1 for 10 min. Cell lysates were resolved using SDS–PAGE and transferred to membranes for western blotting with specific antibodies.

cells grown in NDM or DMEM were exposed to increasing concentrations of AG1024 for 24 h (Fig. 1B). The cytotoxic effect of AG1024 was more than 100 times greater on nutrient-deprived PANC-1 cells (NDM IC_{50} 0.055 μM) relative to cells in nutrient-sufficient medium (DMEM IC_{50} 21 μM). In DMEM, 0.3 μM AG1024 did not induce any significant PANC-1 cell death as determined using propidium iodide and annexin V staining and flow cytometry (Fig. 1C). In contrast, 34% of the cells grown in NDM and treated with the same concentration of AG1024 showed propidium iodide-positive/annexin V-negative staining. We compared the cytotoxicity of AG1024 to that of several conventional anticancer drugs, including doxorubicin, 5-fluorouracil and paclitaxel, in PANC-1 cells grown in NDM versus DMEM (Fig. 1D). The cytotoxicity of doxorubicin, 5-fluorouracil and paclitaxel on PANC-1 cells grown in either medium for 24 h was significantly weaker than AG1024. These results demonstrate clearly that AG1024 exhibits preferential cytotoxicity to nutrient-deprived PANC-1 cells.

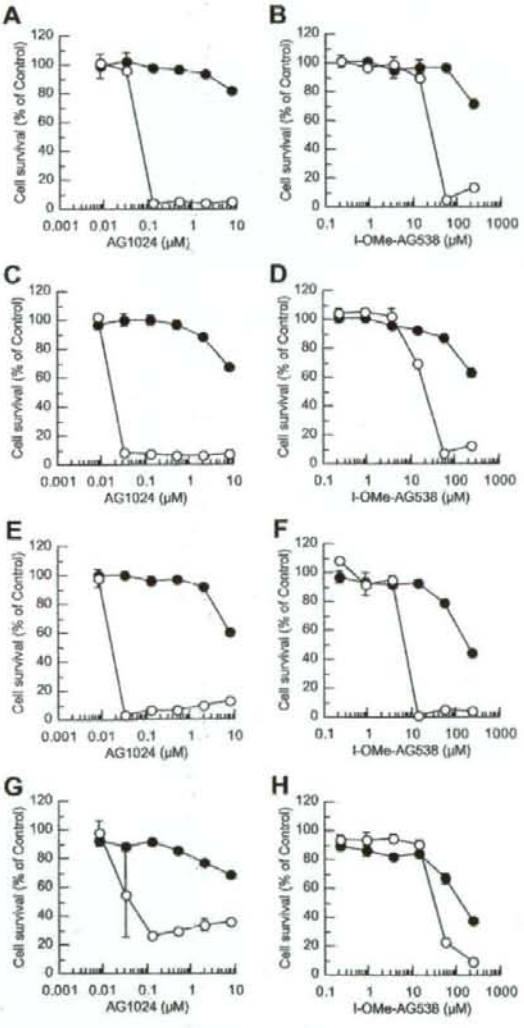

Fig. 4. Effect of AG1024 and I-OMe-AG538 on various human pancreatic cancer cell lines in nutrient-deprived conditions. Human pancreatic cancer cells were incubated with indicated concentrations of AG1024 or I-OMe-AG538 in DMEM (●) or NDM (○) for 24 h. A,B, Capan-1; C,D, MIA Paca-2; E,F, BxPC-3; G,H, PSN-1.

AG1024 inhibits activation of IGF-1R in nutrient-deprived PANC-1 cells

Because AG1024 is a specific inhibitor of IGF-1R kinase, we examined the effect of AG1024 on IGF-1-mediated phosphorylation of IGF-1R in PANC-1 cells grown in different media (Fig. 2). While addition of 0.3 μM AG1024 to PANC-1 cells grown in NDM resulted in a complete inhibition of IGF-1R autophosphorylation, phosphorylation of IGF-1R was only weakly inhibited in cells grown in DMEM with 10-fold higher concentrations of AG1024 (3 μM). AG1024 also inhibited the phosphorylation of Akt (Thr 308), Akt (Ser 473) and Erk, which normally occur as a result of IGF-1R activation. These results demonstrate that AG1024 is a potent inhibitor of IGF-1R activation in nutrient-deprived PANC-1 cells.

I-OMe-AG538 is preferentially cytotoxic to nutrient-deprived PANC-1 cells

In testing whether other IGF-1R inhibitors also functioned preferentially in nutrient-deprived cells, we found that I-OMe-AG538 [23] (another specific inhibitor of IGF-1R, Fig. 3A) also was more cytotoxic to cells in nutrient-deprived medium relative to those in nutrient-sufficient conditions (Fig. 3B). The effect of I-OMe-AG538 on IGF-1R activation in nutrient-deprived cells was similar to AG1024, in that it blocked phosphorylation of IGF-1R, Akt and Erk (Fig. 3C). Our results demonstrate clearly that the IGF-1R inhibitors AG1024 and I-OMe-AG538 both inhibit IGF-1R-mediated signaling and are preferentially cytotoxic to nutrient-deprived PANC-1 cells.

Inhibitors of IGF-1R show preferential cytotoxicity to various human pancreatic cancer cells lines in nutrient-deprived conditions

To determine whether inhibitors of IGF-1R kinase exhibit preferential cytotoxicity to other nutrient-deprived human pancreatic cancer cell lines, we examined the cytotoxic effects of AG1024 and I-OMe-AG538 on Capan-1, MIA Paca-2, BxPC-3, and PSN cells (Fig. 4). AG1024 and I-OMe-AG538 were significantly more cytotoxic to all four human pancreatic cancer cell lines in NDM relative to DMEM, indicating that the cytotoxicity of IGF-1R kinase inhibitors is likely to occur in nutrient-deprived human pancreatic cancer cells. To understand the specificity of IGF-1R kinase inhibitors, we also examined the cytotoxic effects of other representative receptor tyrosine kinase inhibitors (Fig. S1). The cytotoxicities of AG1296 (a PDGFR kinase inhibitor) [24] and AG1478 and PD168393 (EGFR kinase inhibitors) [25–27] were significantly reduced, relative to IGF-1R inhibitors, in both nutrient-deprived and -fed PANC-1 cells. These results indicate that specific inhibition of IGF-1R kinase is important in promoting preferential cytotoxicity in nutrient-starved human pancreatic cancer cells.

Discussion

Tumor microenvironment strongly influences tumor growth and progression. Many aspects of physiology that differentiate solid tumors from normal tissues arise from differences in vasculature. Disorganized vascular systems in tumors result in large areas of tumor exposed to nutrient starvation and hypoxic conditions. In addition, due to the unregulated growth of tumor cells caused by genetic and epigenetic alterations, cells proliferate more rapidly than normal cells and nutrient and oxygen demands often exceeds supply [28–30]. Cancer cells, in particular highly aggres-

sive tumors such as pancreatic cancer that are relatively hypovascular, are able to survive even in conditions of low nutrients and low oxygen supply. Since chronic nutrient deprivation seldom occurs in normal tissues, one strategy for anticancer agent development is to target cancer cells growing in nutrient-deprived conditions. Thus, we screened to identify cytotoxic agents that function preferentially in nutrient-deprived cells.

We found that AG1024, a specific inhibitor of IGF-1R kinase, showed preferential cytotoxicity to human pancreatic cancer PANC-1 cells grown in nutrient-deprived medium. Conventional chemotherapeutic drugs such as doxorubicin, 5-fluorouracil and paclitaxel, were only weakly cytotoxic to nutrient-deprived PANC-1 cells, suggesting that AG1024 may be a unique and attractive starting compound in the development of an antitumor agent. AG1024 has been reported to induce apoptosis in human breast cancer MCF-7 cells [31]. In our present study, flow cytometric analysis showed that AG1024 increased propidium iodide staining without annexin V of nutrient-deprived PANC-1 cells. Kigamicin D and (6a*R*,11a*R*)-3,8-dihydroxy-9-methoxypterocarpan induced necrosis in nutrient-deprived cells [4,32]. Therefore, AG1024 may induce necrosis under nutrient starvation. I-OMe-AG538, another IGF-1R kinase inhibitor that differs in structure from AG1024, was also cytotoxic to nutrient-deprived PANC-1 cells. These IGF-1R kinase inhibitors also were cytotoxic to other nutrient-deprived human pancreatic cancer cell lines, including Capan-1, MIA Paca-2, BxPC-3 and PSN.

IGF-1 binding to the IGF-1R results in activation of receptor tyrosine kinases that stimulates signaling through intracellular networks, including PI3K-AKT-TOR and RAF-MAPK, which then promote cell proliferation and inhibit apoptosis. We found that the IGF-1R kinase inhibitors AG1024 and I-OMe-AG538 blocked phosphorylation of IGF-1R by IGF-1 preferentially in cells cultured in nutrient-deprived conditions relative to those in nutrient-sufficient conditions. These IGF-1R kinase inhibitors also suppressed phosphorylation of Akt and Erk, demonstrating that activation of pathways downstream of the IGF-1R were also blocked in nutrient-deprived conditions.

Unlike AG1296 (a PDGFR kinase inhibitor) or AG1478 and PD168393 (EGFR kinase inhibitors), which are less cytotoxic in nutrient-deprived PANC-1 cells, preferential inhibition of IGF-1 signaling by IGF-1R kinase inhibitors suggests that this pathway may play an important role in cell survival in stress conditions such as nutrient deprivation. The Akt pathway, which functions downstream of IGF-1R, plays a critical role in the proliferation, survival, motility, morphology and therapeutic resistance of cancer cells [33,34]. Because Akt has been demonstrated to regulate cell survival in various stress conditions, including nutrient deprivation, this kinase is viewed as a promising target for cancer therapeutics. Akt inhibitors have been developed including PX-316, which shows antitumor activity against human MCF-7 breast cancer and HT-29 colon cancer xenografts in mice [35]. Thus, part of the preferential cytotoxicity of IGF-1R kinase inhibitors in nutrient-deprived conditions may be due to inhibition of Akt activation.

The IGF-1 receptor is universally expressed in various hematologic and solid tumor cells. NVP-ADW742, another specific inhibitor of IGF-1R kinase, has been shown to be a significant antitumor agent in an orthotopic xenograft multiple myeloma model [20]. Oral administration of the IGF-1R kinase-specific inhibitor NVP-AEW541 has been shown to inhibit IGF-1R signaling in tumors and to reduce tumor growth in a xenograft fibrosarcoma model [19]. The potent cytotoxicity of AG1024 and I-OMe-AG538 to pancreatic cancer cell lines deprived of nutrients (simulating a tumor microenvironment) makes IGF-1R a promising target for new drugs that may be developed to treat a broad spectrum of malignant tumors.

Acknowledgments

This work was supported by Grant-in-Aid for the Third-Term Comprehensive 10-Years Strategy for Cancer Control from the Ministry of Health, Labour and Welfare in Japan. We thanks Dr. H. Esumi (National Cancer Center Hospital East, Japan) for helpful advice, Ms. S. Kakuda for technical assistance and Screening Committee of Anticancer Drugs supported by Grant-in-Aid for Scientific Research on Priority Area "Cancer" from the Ministry of Education, Culture, Sports, Science and Technology, Japan for supplying the SCADS inhibitor kit I.

Appendix A. Supplementary data

Supplementary data associated with this article can be found, in the online version, at doi:10.1016/j.bbrc.2009.01.065.

References

[1] D. Li, K. Xie, R. Wolff, J.L. Abbruzzese, Pancreatic cancer, Lancet 363 (2004) 1049–1057.
[2] S. Shore, D. Vimalachandran, M.G. Raraty, P. Ghaneh, Cancer in the elderly: pancreatic cancer, Surg. Oncol. 13 (2004) 201–210.
[3] K. Izuishi, K. Kato, T. Ogura, T. Kinoshita, H. Esumi, Remarkable tolerance of tumor cells to nutrient deprivation: possible new biochemical target for cancer therapy, Cancer Res. 60 (2000) 6201–6207.
[4] J. Lu, S. Kunimoto, Y. Yamazaki, M. Kaminishi, H. Esumi, D. Kigamicin, A novel anticancer agent based on a new anti-austerity strategy targeting cancer cells' tolerance to nutrient starvation, Cancer Sci. 95 (2004) 547–552.
[5] S. Kunimoto, J. Lu, H. Esumi, Y. Yamazaki, N. Kinoshita, Y. Honma, M. Hamada, M. Ohsono, M. Ishizuka, T. Takeuchi, D. Kigamicins, Novel antitumor antibiotics. I. Taxonomy, isolation, physico-chemical properties and biological activities, J. Antibiot. 56 (2003) 1004–1011.
[6] S. Kunimoto, T. Someno, Y. Yamazaki, J. Lu, H. Esumi, H. Naganawa, D. Kigamicins, Novel antitumor antibiotics. II. Structure determination, J. Antibiot. 56 (2003) 1007–1012.
[7] H. Esumi, J. Lu, Y. Kurashima, T. Hanaoka, Antitumor activity of pyrvinium pamoate, 6-(dimethylamino)-2-[2-(2,5-dimethyl-1-phenyl-1H-pyrrol-3-yl)ethenyl]-1-methyl-quinolinium pamoate salt, showing preferential cytotoxicity during glucose starvation, Cancer Sci. 95 (2004) 685–690.
[8] M.N. Pollak, E.S. Schernhammer, S.E. Hankinson, Insulin-like growth factors and neoplasia, Nat. Rev. Cancer 4 (2004) 505–518.
[9] A. Ullricha, J. Schlessingerb, Signal transduction by receptors with tyrosine kinase activity, Cell 61 (1990) 203–212.
[10] P.V.D. Geer, T. Hunter, R.A. Lindberg, Receptor protein-tyrosine kinases and their signal transduction pathways, Annu. Rev. Cell Biol. 10 (1994) 251–337.
[11] R. Baserga, The contradictions of the insulin-like growth factor 1 receptor, Oncogene 19 (2000) 5574–5581.
[12] E.A. Bohula, A.J. Salisbury, M. Sohail, M.P. Playford, J. Riedemann, E.M. Southern, V.M. Macaulay, The efficacy of small interfering RNAs targeted to the type 1 insulin-like growth factor receptor (IGF1R) is influenced by secondary structure in the IGF1R transcript, J. Biol. Chem. 278 (2003) 15991–15997.
[13] E.K. Maloney, J.L. McLaughlin, N.E. Dagdigian, L.M. Garrett, K.M. Connors, X.-M. Zhou, W.A. Blättler, T. Chittenden, R. Singh, An anti-insulin-like growth factor I receptor antibody that is a potent inhibitor of cancer cell proliferation, Cancer Res. 63 (2003) 5073–5083.
[14] D. Burtrum, Z. Zhu, D. Lu, D.M. Anderson, M. Prewett, D.S. Pereira, R. Bassi, R. Abdullah, A.T. Hooper, H. Koo, X. Jimenez, D. Johnson, R. Apblett, P. Kussie, P. Bohlen, L. Witte, D.J. Hicklin, D.L. Ludwig, A fully human monoclonal antibody to the insulin-like growth factor I receptor blocks ligand-dependent signaling and inhibits human tumor growth in vivo, Cancer Res. 63 (2003) 8912–8921.
[15] P. Hayry, M. Myllarniemi, E. Aavik, S. Alatalo, P. Aho, S. Yilmaz, A.R. Sokolowski, G. Cozzone, B. Jameson, R. Baserga, Stabile D-peptide analog of insulin-like growth factor-1 inhibits smooth muscle cell proliferation after carotid ballooning injury in the rat, FASEB J. 9 (1995) 1336–1344.
[16] D. Sachdev, J.S. Hartell, A.V. Lee, X. Zhang, D. Yee, A dominant negative type I insulin-like growth factor receptor inhibits metastasis of human cancer cells, J. Biol. Chem. 279 (2004) 5017–5024.
[17] C.-T. Lee, K.-H. Park, Y. Adachi, J.Y. Seol, C.-G. Yoo, Y.W. Kim, S.K. Han, Y.-S. Shim, K. Coffee, M.M. Dikov, D.P. Carbone, Recombinant adenoviruses expressing dominant negative insulin-like growth factor-I receptor demonstrate antitumor effects on lung cancer, Cancer Gene. Ther. 10 (2003) 57–63.
[18] Y. Min, Y. Adachi, H. Yamamoto, H. Ito, F. Itoh, C.-T. Lee, S. Nadaf, D.P. Carbone, K. Imai, Genetic blockade of the insulin-like growth factor-I receptor: a promising strategy for human pancreatic cancer, Cancer Res. 63 (2003) 6432–6441.
[19] C. García-Echeverría, M.A. Pearson, A. Marti, T. Meyer, J. Mestan, J. Zimmermann, J. Gao, J. Brueggen, H.-G. Capraro, R. Cozens, D.B. Evans, D.

Fabbro, P. Furet, D.G. Porta, J. Liebetanz, G. Martiny-Baron, S. Ruetz, F. Hofmann, In vivo antitumor activity of NVP-AEW541—a novel, potent, and selective inhibitor of the IGF-IR kinase, Cancer Cell 5 (2004) 231–239.
[20] C.S. Mitsiades, N.S. Mitsiades, C.J. McMullan, V. Poulaki, R. Shringarpure, M. Akiyama, T. Hideshima, D. Chauhan, M. Joseph, T.A. Libermann, C. García-Echeverría, M.A. Pearson, F. Hofmann, K.C. Anderson, Andrew L. Kung, Inhibition of the insulin-like growth factor receptor-1 tyrosine kinase activity as a therapeutic strategy for multiple myeloma, other hematologic malignancies, and solid tumors, Cancer Cell 5 (2004) 221–230.
[21] T. Mosmann, Rapid colorimetric assay for cellular growth and survival: application to proliferation and cytotoxicity assays, J. Immunol. Methods 65 (1983) 55–63.
[22] B. Wen, E. Deutsch, E. Marngoni, V. Frascona, L. Maggiorella, B. Abdulkarim, N. Chavaudra, J. Bourhis, Tyrphostin AG 1024 modulates radiosensitivity in human breast cancer cells, Br. J. Cancer 85 (2001) 2017–2021.
[23] G. Blum, A. Gazit, A. Levitzki, Substrate competitive inhibitors of IGF-1 receptor kinase, Biochemistry 39 (2000) 15705–15712.
[24] L.M. Strawn, G. McMahon, H. App, R. Schreck, W.R. Kuchler, M.P. Longhi, T.H. Hui, C. Tang, A. Levitzki, A. Gazit, I. Chen, G. Keri, L. Orfi, W. Risau, I. Flamme, A. Ullrich, K.P. Hirth, I.K. Shawver, Flk-1 as a target for tumor growth inhibition, Cancer Res. 56 (1996) 3540–3545.
[25] A. Levitzki, A. Gazit, Tyrosine kinase inhibition: an approach to drug development, Science 267 (1995) 1782–1788.
[26] R. Bose, H. Molina, A.S. Patterson, J.K. Bitok, B. Periaswamy, J.S. Bader, A. Pandey, P.A. Cole, Phosphoproteomic analysis of Her2/neu signaling and inhibition, Proc. Natl. Acad. Sci. USA 103 (2006) 9773–9778.
[27] D.W. Fry, A.J. Bridges, W.A. Denny, A. Doherty, K.D. Greis, J.L. Hicks, K.E. Hook, P.R. Keller, W.R. Leopold, J.A. Loo, D.J. McNamara, J.M. Nelson, V. Sherwood, J.B. Smaill, S. Trumpp-Kallmeyer, E.M. Dobrusin, Specific, irreversible inactivation of the epidermal growth factor receptor and erbB2, by a new class of tyrosine kinase inhibitor, Proc. Natl. Acad. Sci. USA 95 (1998) 12022–12027.
[28] C.V. Dang, G.L. Semenza, Oncogenic alterations of metabolism, Trends Biochem. Sci. 24 (1999) 68–72.
[29] R.M. Southerland, Cell and environment interactions in tumor microregions: the multicell spheroid model, Science 240 (1988) 178–184.
[30] G. Helmlinger, F. Yuan, M. Dellian, R.K. Jain, Interstitial pH and pO_2 gradients in solid tumors in vivo: high-resolution measurements reveal a lack of correlation, Nat. Med. 3 (1997) 177–182.
[31] P. Marcelina, G. Aviv, L. Alexander, W. Efrat, L. Derek, Specific inhibitor of insulin-like growth factor-1 and insulin receptor tyrosine kinase activity and biological function by tyrphostins, Endocrinology 138 (1997) 1427–1433.
[32] S. Awale, F. Li, H. Onozuka, H. Esumi, Y. Tezuka, S. Kadota, Constituents of Brazilian red propolis and their preferential cytotoxic activity against human pancreatic PANC-1 cancer cell line in nutrient-deprived condition, Bioorg. Med. Chem. 16 (2008) 181–189.
[33] A. Toker, M. Yoeli-Lerner, Akt signaling and cancer: surviving but not moving on, Cancer Res. 66 (2006) 3963–3966.
[34] A.G. Bader, S. Kang, L. Zhao, P.K. Vogt, Oncogenic PI3K deregulates transcription and translation, Nat. Rev. Cancer 5 (2005) 921–929.
[35] E.J. Meuillet, N. Ihle, A.F. Baker, J.M. Gard, C. Stamper, R. Williams, A. Coon, D. Mahadevan, B.L. George, L. Kirkpatrick, G. Powis, In vivo molecular pharmacology and antitumor activity of the targeted Akt inhibitor PX-316, Oncol. Res. 14 (2004) 513–527.

Autophagy is activated in pancreatic cancer cells and correlates with poor patient outcome

Satoshi Fujii,[1] Shuichi Mitsunaga,[2] Manabu Yamazaki,[1] Takahiro Hasebe,[3] Genichiro Ishii,[1] Motohiro Kojima,[1] Taira Kinoshita,[4] Takashi Ueno,[5] Hiroyasu Esumi[6] and Atsushi Ochiai[1,7]

[1]Pathology Division, Research Center for Innovative Oncology, National Cancer Center Hospital East, 6-5-1 Kashiwanoha, Kashiwa, Chiba 277-8577; [2]Division of Hepatobiliary and Pancreatic Oncology, National Cancer Center Hospital East, 6-5-1 Kashiwanoha, Kashiwa, Chiba 277-8577; [3]Office for Pathology Consultation and Service, Clinical Trials and Practice Support Division, Center for Cancer Control and Information Services, National Cancer Center, 5-1-1, Tsukiji, Chuo-ku, Tokyo 104-0045; [4]Department of Hepatobiliary-Pancreatic Surgery, National Cancer Center Hospital East, 6-5-1 Kashiwanoha, Kashiwa, Chiba, 277-8577; [5]Department of Biochemistry, Juntendo University School of Medicine, 2-1-1 Hongo, Bunkyo-ku, Tokyo 113-8421; [6]Cancer Physiology Project, Research Center for Innovative Oncology, National Cancer Center Hospital East, 6-5-1 Kashiwanoha, Kashiwa, Chiba 277-8577, Japan

(Received April 5, 2008/Revised May 24, 2008/Accepted May 27, 2008/Online publication July 4, 2008)

Because autonomous proliferating cancer cells are often exposed to hypoxic conditions, there must be an alternative metabolic pathway, such as autophagy, that allows them to obtain energy when both oxygen and glucose are depleted. We previously reported finding that autophagy actually contributes to cancer cell survival in colorectal cancers both *in vitro* and *in vivo*. Pancreatic cancer remains a devastating and poorly understood malignancy, and hypoxia in pancreatic cancers is known to increase their malignant potential. In the present study archival pancreatic cancer tissue was retrieved from 71 cases treated by curative pancreaticoduodenectomy. Autophagy was evaluated by immunohistochemical staining with anti-LC3 antibody, as LC3 is a key component of autophagy and has been used as a marker of autophagy. The results showed that strong LC3 expression in the peripheral area of pancreatic cancer tissue was correlated with a poor outcome ($P = 0.0170$) and short disease-free period ($P = 0.0118$). Two of the most significant correlations among the clinicopathological factors tested were found between the peripheral intensity level of LC3 expression and tumor size ($P = 0.0098$) or tumor necrosis ($P = 0.0127$). Activated autophagy is associated with pancreatic cancer cells, and autophagy is thought to be a response to factors in the cancer microenvironment, such as hypoxia and poor nutrient supply. This is the first study to report the clinicopathological significance of autophagy in pancreatic cancer. (*Cancer Sci* 2008; 99: 1813–1819)

Cancers are abnormal tissue masses whose growth exceeds and is uncoordinated with that of adjacent normal tissues, and which persist in the same excessive manner after cessation of the stimulus that evoked them.[1] All cancers ultimately depend on the host for their nutrition and blood supply, but as the preexisting vasculature is obviously insufficient to support the cancers' unlimited requirements for energy and nutrition as a result of their unregulated growth, angiogenesis has been considered pivotal to providing proliferating cancer cells with an adequate source of oxygen, energy, and nutrients. However, recent studies have revealed that even after new blood vessels have formed, both the oxygen and glucose supply is insufficient for the aggressively proliferating cancer cells in locally advanced cancers.[2–4] Tumor hypoxia has been used as a marker of poor prognosis;[5,6] however, how cancer cells become more malignant or survive with an extremely poor blood supply, as for example in pancreatic cancer, is poorly understood.[7] When cancer cells are exposed to hypoxia, anaerobic glycolysis increases and provides energy for cell survival, but as the glucose supply is also insufficient because of the poor blood supply, there must be an alternative metabolic pathway that provides energy when both oxygen and glucose are depleted.[8,9] We have reported that several cancer cell lines, including pancreatic cancer- and colorectal cancer-derived cell lines, are resistant to nutrient-deprived conditions. We have named this starvation-resistant phenotype 'austerity' and speculated that austerity may contribute to cancer cell survival in a nutrient-deficient microenvironment.[8,9]

Autophagy has long been known to be a non-specific self-degradation mechanism that is triggered by nutrient deprivation, but recently it has been shown to play an important role in removing redundant or faulty cell components, such as damaged mitochondria and other organelles that are targeted for lysosomal degradation.[10] The autophagic process occurs in three steps: (1) autophagosome formation; (2) lysosomal fusion with the autophagosome; and (3) lysosomal degradation. In step 1, a cup-shaped lipid bilayer called the isolation membrane is formed and engulfs cytosolic components, including organelles. In step 2, the isolation membrane closes, forming an autophagosome. Cytosolic LC3 (microtubule-associated protein 1 light chain 3), a mammalian homolog of yeast ATG8, is converted to LC3-I (soluble unlipidated form of LC3) during this step and LC3-I is then modified to form LC-3-II (a membrane-bound form) and becomes localized on autophagosomes. Autophagosomes fuse with lysosomes to form autolysosomes. In step 3, the contents of the autolysosomes are degraded rapidly by lysosomal hydrolases, including cathepsins B, D, and L. Intra-autophagosomal LC3-II is also degraded at the same time.[11] Thus, LC3 is a key component of autophagy, and it has been used as a marker of autophagy.

Pancreatic cancer remains a devastating and poorly understood malignancy. Its poor prognosis has been attributed to the inability to make a diagnosis while the tumor is still resectable and a propensity toward early vascular dissemination and spread to regional lymph nodes. Up to 60% of patients have advanced pancreatic cancer at the time of diagnosis, and their median survival time is a dismal 3–6 months.[12] Several pathological features, including tumor size, tumor grade, nodal metastasis, lymphatic or vascular infiltration, and perineural invasion, have been reported to be prognostic pathological parameters for patients with invasive ductal carcinoma (IDC) of the pancreas.[13–20] However, their prognostic value has been a matter of controversy because the studies were based on relatively small numbers of IDC patients. Hypoxia in pancreatic cancer has been reported to increase its malignant potential.[5,6] Studies investigating associations between tumor necrosis in IDC and expression of hypoxic markers, such as hypoxia-inducible factor-1α or carbonic anhydrase IX (CA IX), are expected to provide useful information concerning hypoxia-driven angiogenesis in IDC of the pancreas.[21–23] However, most tissue samples of IDC of the pancreas have been found to be relatively hypovascular compared with the surrounding pancreatic tissue.[7] Proliferating cancer cells require more nutrients

[7]To whom correspondence should be addressed. E-mail: aochiai@east.ncc.go.jp

doi: 10.1111/j.1349-7006.2008.00893.x

than surrounding non-cancerous cells do, though nutrition is supplied via functionally structurally immature neovessels. In other words, because autonomous proliferating cancer cells are often exposed to hypoxic conditions, autophagy is a marker of malignant transformation under hypoxic stress. We speculate that the important process for cancer cells might be autophagy as hypoxia in pancreatic cancer has been reported to be a marker of poor prognosis.[5,6]

Experimental evidence supports a role for autophagy in both cancer development and suppression. Because autophagy-specific genes promote the survival of normal cells during nutrient starvation in all eukaryotic organisms, autophagy may support the survival of rapidly growing cancer cells that have outgrown their vascular supply and are exposed to an inadequate oxygen supply or metabolic stress. By contrast, excessive levels of autophagy promote cell death, presumably via self-cannibalization. Antitumor effects are observed at all levels of autophagy, in the form of either cell death (when the autophagy level is very low or very high) or cell death-independent tumor-suppressor effects (when the autophagy level is intermediate).[24] There might be a balance between the autophagy level and survival of rapidly growing cancer cells if autophagy were turned on or off, according to the nutritional status of cancer cells during the processes of growth, invasion, and metastasis. In a previous study, we showed that autophagosomes are produced actively and consumed promptly in colorectal cancer cells during amino acid starvation, and autophagosome formation was seen only in the tumor cells, never in the adjacent non-cancerous cells. In other words, we found that active autophagy contributes to cancer cell survival in colorectal cancers both *in vitro* and *in vivo*.[25]

It is easy to speculate that the pathophysiological role of autophagy in proliferating cancer cells varies with the type of cancer cell. Autophagy is thought to react to the cancer microenvironment, such as hypoxia and low nutrient supply. There have been no reports of studies on how autophagy functions in cancer tissue, comprising cancer cells and their microenvironment. In the present study we extended our investigation to an *in vivo* study of pancreatic cancer tissue and to elucidating the significance of autophagy in cancer tissue.

Materials and Methods

Patients. The subjects of this study were 71 patients who underwent curative pancreaticoduodenectomy at the National Cancer Center Hospital East, Chiba, Japan between December 1992 and February 2004. The pathological diagnosis in every case was IDC of the pancreas. The median age of the patients was 65 years (mean age 64.3 years), and 31 patients were women. None of the patients received neo-adjuvant therapy before the operation. Regional lymph node dissection was carried out in all patients. None of the 71 patients received adjuvant therapy. All patients agreed to enrollment in the study and each gave informed consent. The institutional review board of the National Cancer Center approved all protocols on the patients' agreements.

Pathological examination. The resected specimens were fixed in 10% formalin at room temperature, and the size and gross appearance of the tumors were recorded. The entire tumor was sectioned at intervals of approximately 0.5 cm, and all tumor-containing sections were processed routinely and embedded in paraffin. Serial sections of each tumor were cut and stained with hematoxylin–eosin, and then examined to confirm the pathological diagnosis. Elastica staining was used to examine them for blood vessel infiltration.

Clinicopathological parameters. The prognostic value of the following histological parameters was assessed in the present study: (1) age (≥65 vs <65 years); (2) sex; (3) tumor size (≥3 vs <3 cm); (4) predominant differentiation of the tumor (well, moderately, or poorly differentiated); (5) lowest degree of tumor differentiation (well, moderately, or poorly differentiated); (6) lymphatic vessel infiltration (≥2 [score 2 or 3] vs <2 [score 0 or 1]); (7) blood vessel infiltration (≥2 [score 2 or 3] vs <2 [score 0 or 1]); (8) intrapancreatic neural invasion (≥2 [score 2 or 3] vs <2 [score 0 or 1]); (9) retroperitoneal invasion (absent vs present); (10) International Union Against Cancer (UICC) pathological T (pT) category (pT1, pT2, or pT3); (11) UICC pathological N (pN) category (pN0 vs pN1); (12) UICC pathological stage (pStage) (≥pStageIIB vs ≤pStageIIA); (13) tumor necrosis (absent vs present); and (14) nerve plexus invasion (absent vs present).[26] Fourteen histological parameters were evaluated in this study according to the UICC,[26] World Health Organization,[27] and the Japan Pancreas Society.[28] Predominant and lowest differentiation was evaluated according to the World Health Organization classification.[27] Tumor necrosis was defined as confluent cell death in invasive areas of primary cancers, visible at an objective lens magnification of ×4.[20]

Outcome. All 71 patients were followed for survival, and the follow-up period was measured from the date of surgery to 29 November 2004. The median follow-up period was 371 days. Overall, 34 patients were diagnosed with local recurrence, 31 patients with liver metastasis, and nine patients with peritoneal metastasis during the follow-up period. Fifty-eight patients died of their disease. Recurrence was defined as initial tumor recurrence. Metastasis or local recurrence was considered as evidence of tumor relapse, and only deaths from pancreatic cancer were considered for the purposes of this study.

Immunohistochemical staining. The method of production of rabbit polyclonal LC3 antibody and of immunohistochemical staining for LC3 have been described previously.[25,29] Formalin-fixed, paraffin-embedded tissue sections containing the maximal cancer tissue area were processed for immunohistochemical staining to enable evaluation of the several clinicopathological factors described below. Some representative cases were used for immunohistochemical staining using rabbit polyclonal CA IX antibody (1 : 50 dilution) (H-120; sc-25599; Santa Cruz Biotechnology) as a hypoxia marker,[21] to examine whether the tumor cells with enhanced LC3 expression were under hypoxic stress.

Evaluation of LC3 expression level by immunohistochemical staining using LC3 antibody. Because nerve cells stain positive for LC3 immunohistochemically,[25] we used the immunohistochemical staining of nerve cells in the tissue as an internal positive control to validate the immunohistochemical staining in each case. Cancer cells whose staining intensity was equal to or stronger than that of nerve cells were judged to be strongly positive, whereas those whose staining was clearly weaker than that of the nerve cells were judged to be weakly positive. Cancer cells that did not stain positively for LC3 immunohistochemically despite a positive internal control were judged to be negative. We selected sections containing the maximal cancer tissue area that included the center of the cancer tissue and the periphery and invasive border between the cancer tissue and non-cancerous tissue. The midpoint between the margin and the center of the cancer tissue was defined as the border between the 'peripheral area' or 'central area'. In other words, the area outside the border and the area inside the border were defined as the peripheral area or the central area, respectively. Thus, the peripheral area contained the invasive border of cancer tissue. Figure 1 shows a schema of how the central area and the peripheral area were defined for each tumor.

The dominant intensity level of LC3-positive cells was evaluated in each central area and peripheral area as follows. The level of intensity of LC3 staining in each area was determined by the percentage of cells that stained negative, weakly positive, and strongly positive. When more than 50% of the LC3-positive cancer cells were strongly positive for LC3 in each area (peripheral area and central area), the area was evaluated as strongly positive, and when more than 50% of the LC3-positive cancer cells were weakly positive for LC3, the area was designated weakly positive.

doi: 10.1111/j.1349-7006.2008.00893.x

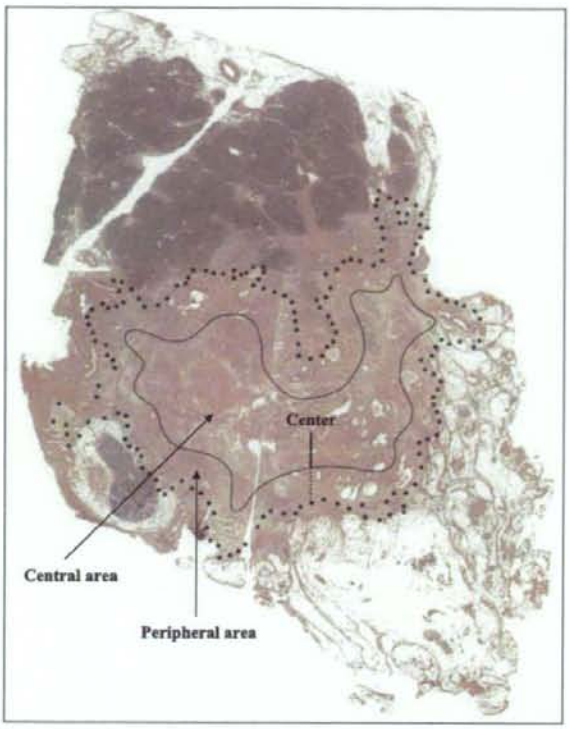

Fig. 1. The central area and the peripheral area of the pancreatic cancer tissue. We mapped the margin of the tumor tissue area of each case and drew a bold dotted line surrounding the tumor tissue area using some slides covering the entire tumor tissue. The margin of tumor tissue is shown as the bold dotted line. The center is decided from the overview. The midpoint between the margin and the center of the cancer tissue was defined as the border between the 'peripheral area' or 'central area'. As shown, the diameter (a small-dotted straight black line) from the marginal bold dotted line of the tumor tissue to the border line and the diameter (a black straight line) from the border line to the center of the tumor tissue were the same. The border line (a black curved line) was drawn so that the diameters were almost the same inside the tumor tissue area. In other words, the area outside the border and the area inside the border were defined as the 'peripheral area' and the 'central area', respectively. Thus, the peripheral area contained the invasive border of cancer tissue.

The cases were classified into three groups according to the dominant overall intensity of the cancer tissue: negative, weakly positive, or strongly positive. The dominant overall intensity in each case was determined according to the predominant intensity of LC3 positivity. When 30% of the cancer cells were weakly positive and 40% were strongly positive, the predominant intensity was recorded as strongly positive. One pathologist (S.F.) evaluated all of the immunohistochemical slides in the present study, and other pathologists (M.Y. and A.O.) also evaluated them to validate the reproducibility of immunohistochemical analyses.

The LC3 immunohistochemical staining factors were analyzed statistically to examine the relationship between clinicopathological factors, overall survival, and disease-free survival.

Statistical analysis. All methods of statistical analysis have been described in a previous report.[20] Overall survival curves and disease-free survival curves were drawn using the Kaplan–Meier method. During the overall survival and disease-free survival periods, significant differences in the levels of LC3 expression that were classified into two or three categories were examined using the log-rank test. In the present study, the clinicopathological factors of pancreatic cancer were classified into two groups similar to the previous study.[20] The relationships between the level of LC3 expression and clinicopathological factors were examined using the χ^2-test. The clinicopathological factors that were significantly associated with the expression level of LC3 in the peripheral area were further analyzed together in multivariate analyses using the Cox proportional hazard regression model to identify the factors that were most significantly associated with the tumor progression of pancreatic cancer. The P-values were two-sided, and the significance level was set at $P < 0.05$. All analyses were carried out using the Statview-J 5.0 package, Windows version (SAS).

Results

LC3 is expressed in pancreatic cancer tissue. As imaging analyses of pancreatic cancer *in vivo* have shown that cancer tissue is more hypovascular than the surrounding non-cancerous tissue,[7] it is speculated that cancer cells use autophagy as a means of nutrition. We evaluated autophagy in surgically resected pancreatic cancer tissue by immunohistochemical staining with anti-LC3 antibody. Formalin-fixed and paraffin-embedded tissue samples from 71 cases of IDC were processed for immunohistochemical analysis, and LC3 expression in the cancer tissue was assessed by comparing it with the staining intensity of nerve cells in intra- or peripancreatic tissue, which expresses LC3 consistently (Figs 2,3). Most pancreatic cancer tissues stained positively for LC3. Weakly or strongly positive expression of LC3 was observed in 62 of the 71 cases of IDC of the pancreas, but there were no positive cells in the cancer tissue from the other nine cases. Table 1 compares the intensity of LC3 expression between the peripheral area and central area of the pancreatic cancer tissue. Intensity in the peripheral area was negative, weakly positive, and strongly positive in nine cases (12.7%), 23 cases (32.4%) and 39 cases (54.9%), respectively. The peripheral area of the pancreatic cancer tissue was strongly positive for LC3 expression in more than half of the cases examined in the present study. The intensity in the central area was negative, weakly positive, and strongly positive in 17 cases (23.9%), 33 cases (46.5%), and 21 cases (29.6%), respectively. The dominant overall intensity of LC3 expression (the most representative level of intensity in the cancer tissue as a whole) was negative, weakly positive, and strongly positive in nine cases (12.7%), 31 cases (43.65%), and 31 cases (43.65%), respectively (Table 1). Thus, the number of cases in which the individual cancer cells were weakly or strongly positive for LC3 was the same as the number of cases counted from the view of dominant overall intensity of LC3 expression.

We examined the difference in intensity level of LC3 expression in the peripheral area and central area of the pancreatic cancer tissue from all 71 cases (Table 2). We classified the pattern of intensity level into three groups according to whether the peripheral or central area contained more cells that stained immunohistochemically positive for LC3: (1) peripheral > central; (2) peripheral = central; and (3) peripheral < central. The peripheral intensity level of LC3 staining was stronger in 25 (40.3%) of the 62 cases that were positive for LC3 expression, and weaker in only two cases (3.2%), and LC3 expression in the peripheral area and central area was the same in 35 cases (56.5%). There was a trend toward a stronger level of intensity of LC3 expression in the peripheral area of the pancreatic cancer tissue, which included the invasive border.

To address the question of whether peripheral tumor cells with enhanced LC3 expression are under hypoxic stress, we carried out immunohistochemical staining using CA IX as a hypoxia marker on some representative cases. The results showed that in some cases the tumor cells with strong LC3 expression at the peripheral area concomitantly showed enhanced expression of CA IX (Fig. 4).

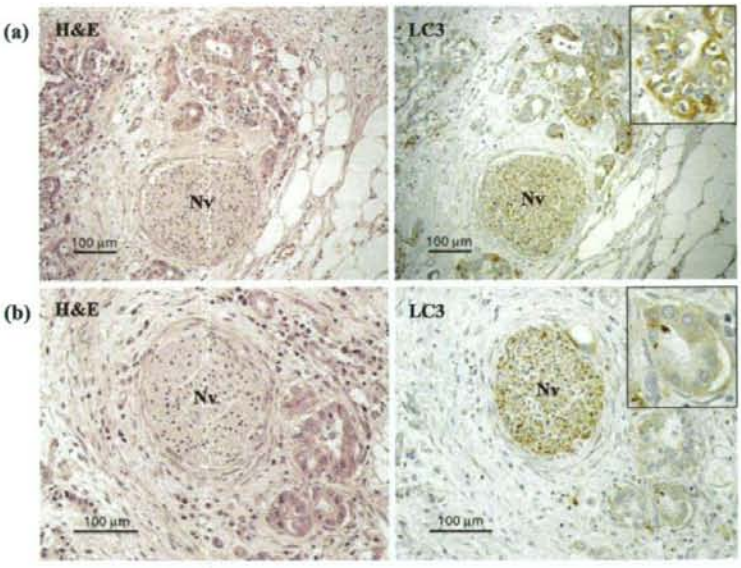

Fig. 2. LC3 protein was detected in pancreatic cancer tissue by immunohistochemical staining with LC3 antibody. Cancer tissue stained immunohistochemically with LC3 antibody and corresponding hematoxylin–eosin (HE)-stained sections are shown. A nerve cell (Nv) was used as an internal positive control to validate immunohistocheimical staining and evaluate the level of intensity of LC3 expression. The inserts are the photographs at higher magnification. (a) The cancer cells that stained as or more intensely for LC3 than the nerve cells were recorded as strongly positive. (b) The cancer cells that stained less intensely for LC3 than the nerve cells were recorded as weakly positive.

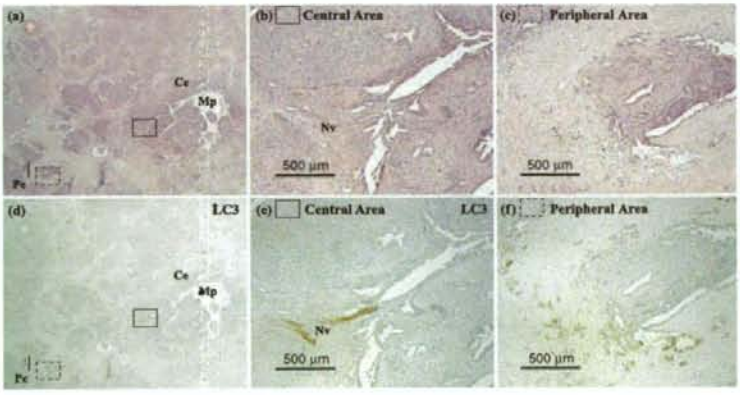

Fig. 3. A representative pancreatic tumor is shown. Cancer tissue (d–f) stained immunohistochemically with LC3 antibody and (a–c) corresponding hematoxylin–eosin (HE)-stained sections are shown. The peripheral area of the pancreatic cancer tissue (Pe) is more strongly positive for LC3 protein than the central area (Ce). Mp, main pancreatic duct; Nv, nerve cell.

Table 1. Intensity level of LC3 expression between the peripheral area and central area of the pancreatic cancer tissue, and the dominant overall intensity of LC3 expression of the pancreatic cancer tissue

Staining	Dominant intensity in the peripheral area (%)	Dominant intensity in the central area (%)	Dominant overall intensity (%)
Negative	9 (12.7)	17 (23.9)	9 (12.7)
Weakly positive	23 (32.4)	33 (46.5)	31 (43.65)
Strongly positve	39 (54.9)	21 (29.6)	31 (43.65)
Total cases	71 (100)	71 (100)	71 (100)

Table 2. Differences in the intensity level of LC3 expression in the peripheral area and central area of the pancreatic cancer tissue

No. cases	Pattern of intensity level		
	Peripheral > central (%)	Peripheral = central (%)	Peripheral < central (%)
62	25 (40.3)	35 (56.5)	2 (3.2)

Strong expression of LC3 in the peripheral area of the cancer tissue correlates with poor outcome and a short disease-free period. We analyzed the relationship between the intensity of LC3 expression (negative, weakly positive, strongly positive) in the peripheral area of pancreatic cancer tissue and overall survival. There was a trend toward the group with a strongly positive peripheral area to have a poor outcome ($P = 0.0579$) (Fig. 5a). We speculated that the cells strongly positive for LC3 in the peripheral area of the cancer tissue have a significant role in the characteristics of aggressive pancreas cancers and we divided the cases into two

doi: 10.1111/j.1349-7006.2008.00893.x

Fig. 4 Tumor cells with enhanced LC3 expression at the peripheral area concomitantly expressed carbonic anhydrase IX (CA IX) as a hypoxia marker. Three photographs of a representative case are shown (hematoxylin–eosin and CA IX and LC3 expression by immununohistochemical staining). The black arrows show the peripheral nerve at the peripheral area of the tumor tissue and which served as a positive internal control of LC3 expression.

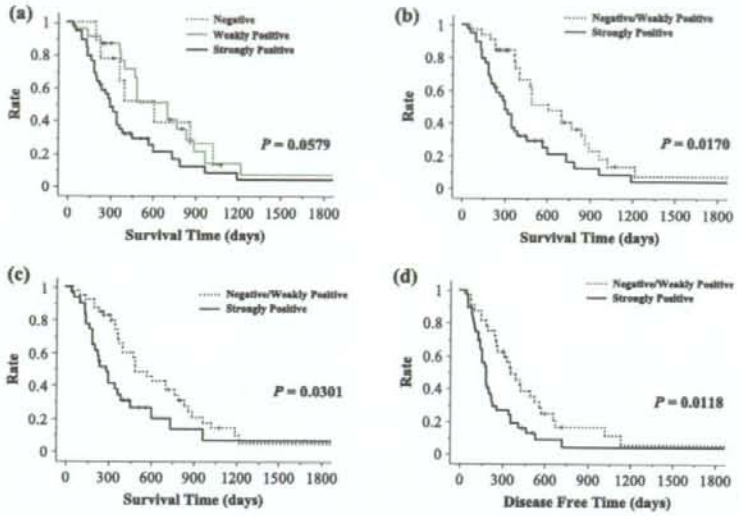

Fig. 5. Overall survival curves and disease-free curve according to the level of intensity of LC3 protein expression in the peripheral area and the dominant overall intensity of LC3 expression. (a) Overall survival curves according to the level of intensity of LC3 expression in the peripheral area of the cancer tissue in a negative group, weakly positive group, and strongly positive group. There was a trend for patients with strongly positive expression of LC3 protein to have a poor outcome ($P = 0.0579$). (b) Overall survival curves according to the level of intensity of LC3 protein expression in the peripheral area of the cancer tissue in the negative and weakly positive group and the strongly positive group. The group with strongly positive expression of LC3 protein had a significantly shorter survival time ($P = 0.0170$). (c) Overall survival curves according to the dominant overall intensity of LC3 protein expression in the negative and weakly positive group and the strongly positive group. The group with strongly positive expression of LC3 protein had a significantly shorter survival time ($P = 0.0301$). (d) Disease-free curves according to the level of intensity of LC3 protein expression in the peripheral area of the cancer tissue in the negative and weakly positive group and the strongly positive group. The group with strongly positive expression of LC3 protein in the peripheral area of the cancer tissue had a significantly shorter disease-free period ($P = 0.0118$).

groups, a negative or weakly positive group and a strongly positive group, according to the results for staining in the peripheral area. Interestingly, there was a significant correlation between the level of intensity of LC3 expression in the peripheral area of the cancer tissue and poor outcome ($P = 0.0170$) (Fig. 5b). Moreover, cases in which the dominant overall intensity of LC3 expression was strongly positive had a poorer outcome than the group in which the dominant overall intensity was weakly positive or negative ($P = 0.0301$) (Fig. 5c). Cases with a strongly positive intensity level in the peripheral area of the cancer tissue had a significantly shorter disease-free period than the cases with a negative or weakly positive intensity level ($P = 0.0118$) (Fig. 5d).

LC3 expression is correlated with clinicopathological factors, including tumor necrosis, differentiation, blood vessel infiltration, and tumor necrosis. In our study, there were significant correlations between a strong intensity of LC3 expression in the peripheral area, which included the invasive border, and a poor outcome and short disease-free survival time. In the next step, we investigated the relationship between LC3 expression and clinicopathological factors, including age, sex, tumor size, predominant differentiation, lowest differentiation, lymphatic vessel infiltration, blood vessel infiltration, intrapancreatic neural invasion, retroperitoneal invasion, UICC pT, UICC pN, UICC pStage, tumor necrosis, and nerve plexus invasion. The results showed significant correlations between the intensity level of LC3 expression in the peripheral area of the tumor and tumor size, predominant differentiation, lowest degree of differentiation, blood vessel infiltration, and tumor necrosis ($P < 0.05$) (Table 3), and two of the most significant correlations were with tumor size ($P = 0.0098$) or tumor necrosis ($P = 0.0127$) (Table 3).

Multivariate analyses of parameters significantly associated with overall survival. We carried out multivariate analyses to investigate the prognostic value of tumor size greater than 3.0 cm, predominantly poor differentiation, lowest degree of differentiation, 2 or 3 degrees of blood vessel infiltration, tumor necrosis and strongly positive intensity at the peripheral area, but only tumor size greater than 3.0 cm significantly increased the hazard ratio for overall survival

Table 3. Relationship between LC3 expression and clinicopathological factors of pancreatic cancer

	No. cases	LC3 expression			*P*-value
		N	W	S	
Age					
<65 years	37	3	10	24	
≥65 years	34	6	13	15	0.1875
Sex					
Male	40	5	13	22	
Female	31	4	10	17	0.9987
Tumor size					
<3.0 cm	34	3	17	14	
≥3.0 cm	37	6	6	25	0.0098
Predominant differentiation					
Well	25	5	13	7	
Moderately	37	3	8	26	0.0227
Poorly	9	1	2	6	
Lowest differentiation					
Well	8	2	5	1	
Moderately	27	2	11	14	0.0431
Poorly	36	5	7	24	
Lymphatic vessel infiltration					
0 or 1	50	6	19	25	
2 or 3	21	3	4	14	0.2940
Blood vessel infiltration					
0 or 1	7	1	5	1	
2 or 3	64	8	18	38	0.0497
Intrapancreatic neural invasion					
0 or 1	20	3	6	11	
2 or 3	51	6	17	28	0.1680
Retroperitoneal invasion					
0 or 1	27	4	12	11	
2 or 3	44	5	11	28	0.1567
UICC pT					
pT1 or pT2	4	1	1	2	
pT3	67	8	22	37	0.7415
UICC pN					
pN0	11	2	5	4	
pN1	60	7	18	35	0.4038
UICC pStage					
IA/IB/IIA	14	2	6	6	
IIB/III/IV	57	7	17	33	0.5805
Tumor necrosis					
Absent	50	7	21	22	
Present	21	2	2	17	0.0127
Nerve plexus invasion					
Absent	26	3	9	14	
Present	45	6	14	25	0.9450

N, negative; S, strongly positive; W, weakly positive.

($P = 0.0018$, hazard ratio = 2.8, 95% confidence interval = 1.4–5.2). None of the other factors significantly increased the hazard ratio for overall survival in the multivariate analyses.

Discussion

The clinicopathological significance of autophagy in cancer progression has remained unclear, and the role of autophagy in cell fate decisions remains a matter of controversy. Autophagy has been regarded as playing a role in providing nutrients by degrading existing cellular components. It is referred to as a recycling of cell constituents and an adaptive response to various cell stresses, such as energy deficiency.[10] Recently, the role of autophagy has also been shown to be an indispensable physiological reaction in caspase-independent programmed cell death (autophagic death), and autophagic cell death has been found to eliminate damaged and harmful cells, such as cancer cells damaged by anticancer reagents and cells infected with pathogenic microorganisms.[30,31] Paradoxically, autophagy has been proposed to be an indispensable physiological reaction for sustaining cell viability under nutrient-starved conditions.[10] In our previous study, we showed that colorectal cancer cells harbor functional autophagic machinery and that the autophagic machinery functions to prolong cell survival during shortages of nutrients.[25] The membrane-bound LC3-II protein level is used as a marker of autophagosome formation. We detected LC3-II by western blotting with the anti-LC3 antibody used in the previous study, and LC3 protein has also been detected in colon cancer cells by immunohistochemical staining.[25] We demonstrated that LC3 protein detected by immunohistochemical staining coincided with the localization of autophagosomes in colon cancer tissue specimens containing LC3 protein by electron microscopy and that autophagy contributes directly to cancer cell survival during nutrient starvation.[25] In a previous experiment, both an autolysosomal protease inhibitor and 3-methyladenine, an inhibitor of autophagosome formation, induced marked apoptotic death in all colorectal cancer cells examined.[25] However, the significance of excess expression of autophagic machinery in cancer tissue samples remained unclear. In the present study we showed that LC3 positivity of pancreatic cancer tissue was correlated with poor overall survival and a shorter disease-free period. Constitutive formation of autophagosomes in cancer cells may contribute to cell survival in the harsh cancer microenvironments in which cancers are known to progress.

On the other hand, autophagy may not be a causal step in malignant transformation at the cellular level and may instead be an indicator of a poor blood supply in the cancer microenvironment.[32] Interestingly, however, significant associations were found between the LC3 expression level in the peripheral area, which included the invasive margin, and several clinicopathological factors, including tumor size, predominant differentiation, lowest differentiation, blood vessel infiltration, and tumor necrosis. Multivariate analyses showed that the LC3 expression level in the peripheral area was not an independent prognostic factor, but that tumor size greater than 3.0 cm, which was the factor most significantly correlated with LC3 expression ($P = 0.0098$, Table 3), was significantly associated with poor overall survival. Moreover, there was a correlation between tumor necrosis and strong expression of LC3 in pancreatic cancer tissue ($P = 0.0127$; Table 3). Two cases showed decreased intensity of LC3 expression by immunohistochemical staining at the peripheral area (Table 2). Both of them showed an absence of tumor necrosis and the sizes of both tumors were less than 3 cm. Nine cases were totally negative for LC3 expression (Table 3). Only two cases (2.8%) were negative for LC3 expression and tumor necrosis, whereas 19 cases (26.8%) were positive for LC3 expression and tumor necrosis. Six cases (8.5%) were negative for LC3 expression and had a tumor size of 3.0 cm ≤ 0. Twenty-five cases (35.2%) were positive for LC3 expression and had a tumor size of ≤3.0 cm. Negative cases showed lesser tumor size (<3.0 cm) and an absence of tumor necrosis with significant correlations. These results suggest the functional significance of autophagy in pancreatic cancer tissue. This observation indicates that autophagy may promote cell viability in hypovascular pancreatic cancer tissue, where only limited oxygen and nutrient supplies would be expected. To address the question of whether peripheral tumor cells with enhanced LC3 expression are under hypoxic stress, we carried out immunohistochemical staining using CA IX as a hypoxia marker on some representative cases. There were some cases whose tumor cells with strong LC3 expression at the peripheral area showed concomitant enhanced expression of CA IX (Fig. 4). However, further studies are needed to address the relationship between autophagy and hypoxia, angiogenesis, and nutrient starvation by investigating a large

doi: 10.1111/j.1349-7006.2008.00893.x

number of cases and many kinds of cancer tissues. No LC3 expression was detected in the non-cancerous ductal epithelium of the pancreas in the present study (data not shown). We do not understand this discrepancy if autophagy is regarded as just a physiological response to poor blood supply. Moreover, as LC3 expression was significantly correlated with various clinicopathological factors, further study will be needed to determine its significance in relation to the malignant character of cancer cells.

Based on all of the above, taken together, we conclude that activated autophagy is associated with pancreatic cancer cells and that LC3 expression by pancreatic cancer cells is significantly correlated with a poor outcome. This is the first study to show the clinicopathological significance of autophagy in relation to a poor outcome and associations with clinicopathological parameters. It is speculated that autophagy may play a variety of pathophysiological roles in carcinogenesis, cancer progression, and metastasis, and that its role may vary with the cancer cell type due to differences in the characters of the cancer cells themselves and the microenvironment of the cancer tissue. To better understand the autophagic machinery for cancer cell survival related to carcinogenesis and cancer progression, we plan to extend our investigation to other cancer cell types by using cancer tissue samples.

Acknowledgments

This work was supported by a grant from the Ministry of Health, Labour, and Welfare for the Third-Term Comprehensive 10-year Strategy for Cancer Control. We wish to thank Miss Mai Okumoto for her excellent technical assistance.

References

1 Kumar V, Cotran RS, Robbins SL. *Robbins Pathologic Basis of Disease*, 5th edn. Philadelphia: W.B. Saunders, 1992.
2 Jain RK. Molecular regulation of vessel maturation. *Nat Med* 2003; **9**: 685–93.
3 Vaupel P, Thews O, Hoeckel M. Treatment resistance of solid tumors: role of hypoxia and anemia. *Med Oncol* 2001; **18**: 243–59.
4 Harris AL. Hypoxia – a key regulatory factor in tumour growth. *Nat Rev Cancer* 2002; **2**: 38–47.
5 Koong AC, Mehta VK, Le QT *et al*. Pancreatic tumors show high levels of hypoxia. *Int J Radiat Oncol Biol Phys* 2000; **48**: 919–22.
6 Buchler P, Reber HA, Lavey RS *et al*. Tumor hypoxia correlates with metastatic tumor growth of pancreatic cancer in an orthotopic murine model. *J Surg Res* 2004; **120**: 295–303.
7 Kitano M, Kudo M, Maekawa K *et al*. Dynamic imaging of pancreatic diseases by contrast enhanced coded phase inversion harmonic ultrasonography. *Gut* 2004; **53**: 854–9.
8 Izuishi K, Kato K, Ogura T, Kinoshita T, Esumi H. Remarkable tolerance of tumor cells to nutrient deprivation: possible new biochemical target for cancer therapy. *Cancer Res* 2000; **60**: 6201–7.
9 Esumi H, Izuishi K, Kato K *et al*. Hypoxia and nitric oxide treatment confer tolerance to glucose starvation in a 5′-AMP-activated protein kinase-dependent manner. *J Biol Chem* 2002; **277**: 32 791–8.
10 Levine B, Klionsky DJ. Development by self-digestion: molecular mechanisms and biological functions of autophagy. *Dev Cell* 2004; **6**: 463–77.
11 Tanida I, Minematsu-Ikeguchi N, Ueno T, Kominami E. Lysosomal turnover, but not a cellular level, of endogenous LC3 is a marker for autophagy. *Autophagy* 2005; **1**: 84–91.
12 Sener SF, Fremgen A, Menck HR, Winchester DP. Pancreatic cancer: a report of treatment and survival trends for 100 313 patients diagnosed from 1985 to 1995, using the National Cancer Database. *J Am Coll Surg* 1985; **189**: 1–7.
13 Geer RJ, Brennan MF. Prognostic indicators for survival after resection of pancreatic adenocarcinoma. *Am J Surg* 1993; **165**: 68–72.
14 Sohn TA, Yeo CJ, Cameron JL *et al*. Resected adenocarcinoma of the pancreas-616 patients: results, outcomes, and prognostic indicators. *J Gastrointest Surg* 2000; **4**: 567–79.
15 Lim JE, Chien MW, Earle CC. Prognostic factors following curative resection for pancreatic adenocarcinoma: a population-based, linked database analysis of 396 patients. *Ann Surg* 2003; **237**: 74–85.
16 Kuhlmann KF, de Castro SM, Wesseling JG *et al*. Surgical treatment of pancreatic adenocarcinoma: actual survival and prognostic factors in 343 patients. *Eur J Cancer* 2004; **40**: 549–58.
17 Luttges J, Schemm S, Vogel I, Hedderich J, Kremer B, Kloppel G. The grade of pancreatic ductal carcinoma is an independent prognostic factor and is superior to the immunohistochemical assessment of proliferation. *J Pathol* 2000; **191**: 154–61.
18 Takai S, Satoi S, Toyokawa H *et al*. Clinicopathologic evaluation after resection for ductal adenocarcinoma of the pancreas: a retrospective, single-institution experience. *Pancreas* 2003; **26**: 243–9.
19 Takahashi S, Hasebe T, Oda T *et al*. Extra-tumor perineural invasion predicts postoperative development of peritoneal dissemination in pancreatic ductal adenocarcinoma. *Anticancer Res* 2001; **21**: 1407–12.
20 Mitsunaga S, Hasebe T, Iwasaki M, Kinoshita T, Ochiai A, Shimizu N. Important prognostic histological parameters for patients with invasive ductal carcinoma of the pancreas. *Cancer Sci* 2005; **96**: 858–65.
21 Kivelä AJ, Parkkila S, Saarnio J *et al*. Expression of transmembrane carbonic anhydrase isoenzymes IX and XII in normal human pancreas and pancreatic tumours. *Histochem Cell Biol* 2000; **114**: 197–204.
22 Shibaji T, Nagao M, Ikeda N *et al*. Prognostic significance of HIF-1 alpha overexpression in human pancreatic cancer. *Anticancer Res* 2003; **23**: 4721–7.
23 Sipos B, Weber D, Ungefroren H *et al*. Vascular endothelial growth factor mediated angiogenic potential of pancreatic ductal carcinomas enhanced by hypoxia: an *in vitro* and *in vivo* study. *Int J Cancer* 2002; **102**: 592–600.
24 Levine B. Cell biology: autophagy and cancer. *Nature* 2007; **446**: 745–7.
25 Sato K, Tsuchihara K, Fujii S *et al*. Autophagy is activated in colorectal cancer cells and contributes to the tolerance to nutrient deprivation. *Cancer Res* 2007; **67**: 9677–84.
26 Sobin HL, Wiitekind C, eds. *TNM Classification of Malignant Tumors*, 6th edn. New York: Wiley-Liss, 2002.
27 Hamilton RS, Aaltonen AL, eds. *World Health Organization Classification of Tumours. Pathology and Genetics of Tumors of the Digestive System*. Lyon: IARC Press, 2000.
28 Japan Pancreas Society. *The Classification of Pancreatic Carcinoma*, 1st English edn. Tokyo: Kanehara, 1996.
29 Jäger S, Bucci C, Tanida I *et al*. Role for Rab7 in maturation of late autophagic vacuoles. *J Cell Sci* 2004; **117**: 4837–48.
30 Kirkegaard K, Taylor MP, Jackson WT. Cellular autophagy: surrender, avoidance and subversion by microorganisms. *Nat Rev Microbiol* 2004; **2**: 301–14.
31 Kondo Y, Kanzawa T, Sawaya R, Kondo S. The role of autophagy in cancer development and response to therapy. *Nat Rev Cancer* 2005; **5**: 726–34.
32 Klionsky DJ, Abeliovich H, Agostinis P *et al*. Guidelines for the use and interpretation of assays for monitoring autophagy in higher eukaryocytes. *Autophagy* 2008; **4**: 151–75.

[Autophagy 4:5, 692-700; 1 July 2008]; ©2008 Landes Bioscience

Research Paper

Loss of Pten, a tumor suppressor, causes the strong inhibition of autophagy without affecting LC3 lipidation

Takashi Ueno,[1] Wataru Sato,[2] Yasuo Horie,[2] Masaaki Komatsu,[1] Isei Tanida,[1,†] Mitsutaka Yoshida,[3] Shigetoshi Ohshima, Tak Wah Mak,[4] Sumio Watanabe[2,‡] and Eiki Kominami[1,*]

[1]The Department of Biochemistry and [3]Division of Ultrastructural Research; Juntendo University School of Medicine; Hongo, Tokyo Japan; [2]The Department of Gastroenterolog Akita University; Akita, Japan; [4]The Campbell Family Institute for Breast Cancer Research; Toronto, Ontario Canada

[†]Present address: Department of Biochemistry and Cell Biology; National Institute of Infectious Disease; Tokyo, Japan

[‡]Present address: Department of Gastroenterology; Juntendo University School of Medicine; Tokyo, Japan

Abbreviations: Pten, phosphatase and tensin homologue deleted on chromosome ten; PI3-kinase, phosphatidylinositol 3-kinase; PtdIn phosphatidylinositol; PtdIns(4,5)P_2, phosphatidylinositol (4,5)-bisphosphate; PtdIns(3,4)P_2,phosphatidylinositol (3,4)-bisphosphat PtdIns(3,4,5)P_3, phosphatidylinositol (3,4,5)-trisphosphate; Akt, protein kinase B; RT, real time; PCR, polymerase chain reaction; FCS, fet calf serum; Williams E/10% FCS, Williams' medium E containing 10% FCS; PBS, 20 mM Na-phosphate, pH 7.4, 0.15 M NaCl; E64c ethyl-(+)-(2S,3S)-3-[(S)-methyl-1-(3methyl-butyl-carbamoyl)-butylcarbamoyl]-2-oxiranecarboxylate; MAP, microtubule associated protei LC3, light chain 3; LC3-I, solubleform of light chain 3; LC3-II, lipidated form of light chain 3; GABARAP, γ-aminobutyric acid$_A$ receptor assoiciated protein; GST, glutathione S-transferase; MBP, maltose binding protein; BHMT, betaine homocysteine methyltransferase; SDS sodium dodecylsulfate; PAGE, polyacrylamide gel electrophoresis; mTor, mammalian target of rapamycin; LGP85, lysosomal membran glycoprotein 85

Key words: autophagy, Pten, autophagosome, autolysosome, class I phosphatidylinositol-3-kinase, Akt

[1]Pten (phosphatase and tensin homolog deleted on chromosome ten), a tumor suppressor, is a phosphatase with a variety of substrate specificities. Its function as a negative regulator of the class I phosphatidyl-inositol 3-kinase/Akt pathway antagonizes insulin-dependent cell signaling. The targeted deletion of Pten in mouse liver leads to insulin hypersensitivity and the upregulation of the phosphatidyl-inositol 3-kinase/Akt signaling pathway. In this study, we investigated the effects of Pten deficiency on autophagy, a major cellular degradative system responsible for the turnover of cell constituents. The autophagic degradation of [^{14}C]-leucine-labeled proteins of hepatocytes isolated from Pten-deficient livers was strongly inhibited, compared with that of control hepatocytes. However, no significant difference was found in the levels of the Atg12-Atg5 conjugate and LC3-II, the lipidated form of LC3, an intrinsic autophagosomal membrane marker, between control and Pten-deficient livers. Electron microsopic analyses showed that numerous autophagic vacuoles (autophagosomes plus autolysosomes) were present in the livers of control mice that had been starved for 48 hours, whereas they were markedly reduced in Pten-deficient livers under the same conditions. In vivo administration of leupeptin to control livers caused the inhibition of autophagi proteolysis, resulting in the accumulation of autolysosomes. Thes autolysosomes could be separated as a denser autolysosom fraction from other cell membranes by Percoll density gradien centrifugation. In leupeptin-administered mutant livers, howeve the accumulation of denser autolysosomes was reduced substan tially. Collectively, we conclude that enhanced insulin signaling i Pten deficiency suppresses autophagy at the formation and matura tion steps of autophagosomes, without inhibiting *ATG* conjugatio reactions.

*Correspondence to: Eiki Kominami; Department of Biochemistry; Juntendo University School of Medicine; Building 9; Rm. 913; 2-1-1 Hongo; Bunkyo-ku, Tokyo 113-8421 Japan; Tel.: +81.3.5802.1030; Fax: +81.3.5802.5889; Email: komilabo@med.juntendo.ac.jp

Submitted: 01/18/08; Revised: 04/09/08; Accepted: 04/10/08

Previously published online as an *Autophagy* E-publication: http://www.landesbioscience.com/journals/autophagy/article/6085

Introduction

Insulin plays a critical role in controlling glucose and lipid metab olism in liver, muscle and adipose tissues. In muscle and adipos tissue, insulin promotes glucose uptake from circulating blood t cells, resulting in a decrease in blood glucose levels. In liver, insuli stimulates glycogen synthesis, glycolysis, fatty acid synthesis an protein synthesis. The binding of insulin to insulin receptors induce a series of complex cell signaling pathways, in which the class I phos phatidylinositol 3-kinase (PI3-kinase)/Akt plays a key role, upstrear in the pathway. The insulin signal causes the activation of class PI3-kinase.[1-3] Activated class I PI3-kinase phosphorylates phosphati dylinositol 4-phosphate and phosphatidylinositol (4,5)-bisphosphat (PtdIns(4,5)P_2) to form phosphatidylinositol (3,4)-bisphosphat (PtdIns(3,4)P_2) and phosphatidylinositol (3,4,5)-trisphosphat (PtdIns(3,4,5)P_3), respectively.[4] Both PtdIns(3,4)P_2 andPtdIns(3,4,5 P_3 bind to Akt (protein kinase B) and its activator phosphoinositide dependent kinase-1.[5,6] Activated Akt is required for the subsequen

inactivation of glycogen synthase kinase 3β, which eventually leads to the stimulation of glycogen synthesis and fatty acid synthesis.[7] Activated Akt also stimulates the mTor /P70S6-kinase pathway, the activation of which is required for the initiation of protein synthesis.[8,9] Pten is a tumor suppressor, with multifunctional phosphatase activity.[10] Pten specifically dephosphorylates PtdIns(3,4,5)P_3 to produce PtdIns(4,5)P_2, thus functioning as a negative regulator of the class I PI3-kinase/Akt pathway.[11] It has been reported that Pten is frequently mutated in many cancer cells. The inactivation of Pten results in hyper activation of the class I PI3-kinase/Akt pathway, which is closely correlated with the dysregulation of cell proliferation.

Autophagy is a catabolic system that plays a major role in the turnover of cell constituents, including organelles and cytosolic proteins.[12,13] Autophagy has been most fully investigated in the liver. Under nutrient-rich conditions, autophagy proceeds at the basal rate (~1.5% of total liver protein/hour). Under starvation conditions, the rate is enhanced ~3-fold to a maximal level (~4–5% of the total liver protein/hour).[14] In nutrient starved cells, numerous autophagosomes engulfing cytoplasmic organelles (mitochondria, endoplasmic reticulum, ribosomes, etc.,) and soluble cytosolic proteins are formed. The autophagosome then fuses with a lysosome to mature into an autolysosome, in which sequestered cytoplasmic components are degraded by lysosomal hydrolases. More than 20 *ATG* genes that are essential for autophagy have been identified and characterized to date.[15,16] Many of the *ATG* genes play pivotal roles in two ubiquitylation-like protein conjugation systems.

Autophagy is distinctly controlled by two different classes of PI3-kinase.[17] The stimulation of class I PI3-kinase activity inhibits autophagy, whereas the class III PI3-kinase that phosphorylates PtdIns to produce PtdIns(3)-phosphate is required for autophagy. It has been reported that feeding HT-29 cells with synthetic lipids dipalmitoyl PtdIns(3,4)P_2 and dipalmitoyl PtdIns(3,4,5)P_3 or the activation of class I PI3-kinase by interleukine 13 causes a significant inhibition in autophagy, whereas feeding synthetic dipalmitoyl PtdIns(3)-phosphate, a class III PI3-kinase product, stimulates autophagy.[18] In fact, the overexpression of wild-type Pten in HT-29 cells reversed the inhibitory effect of autophagy by interleukine 13, whereas the overexpression of a mutant form of Pten, which lacks phosphoinositide phosphatase activity, failed to reverse the inhibition of autophagy.[19] In addition, overexpression of the constitutively active form of Akt in HT-29 cells caused the inhibition of autophagy, whereas the overexpression of the constitutively inactive form of Akt caused the activation of autophagy.[19] These results suggest that the signaling pathway downstream from Akt is important for the negative control of autophagy. In the yeast *Saccharomyces cerevisiae*, PI3-kinase Vps34 forms two distinct protein complexes. One complex, comprised of Vps34/Vps15/Atg6(Vps30)/Vps38, functions in post-Golgi membrane transport and the other complex, comprised of Vps34/Vps15/Atg6(Vps30)/Atg14, functions in autophagy.[20] In mammals, class III PI3-kinase, a mammalian homologue of yeast Vps34, forms a complex with beclin 1(mammalian Atg6 homologue) in the trans Golgi network[21] and this complex formation has been shown to be essential for autophagy.[21,22] In contrast to the essential role of the class III PI3-kinase in autophagy, the molecular mechanism, by which autophagy is inhibited by the class I PI3-kinase, is not fully understood. In particular, little is known as to which of the th steps of autophagy, i.e., autophagosome formation, the maturati of autophagosomes into autolysosomes, and autolysosomal degrad tion, is most affected by the stimulation of the class I PI3-kinase/A pathway. In order to address this issue, we identified an anin model in which the class I PI3-kinase is constitutively activat thus permitting autophagy to be suppressed, irrespective of t nutrient conditions.

Hepatocyte-specific Pten-deficient mice were a useful expe mental system for investigating the effects of hyper activation of t class I PI3-kinase/Akt pathway on metabolism.[23,24] As expected, t loss of Pten function elicited insulin hypersensitivity with eleva levels of phosphorylated Akt and led to tumorigenesis, the develo ment of adenomas and hepatocellular carcinomas.[24] Unexpected the Pten deficiency induced diverse genes that are involved in fa acid synthesis and β-oxidation, resulting in a fatty liver and stea hepatitis with accumulated triglycerides.[23,24] Using this anin model, we investigated the effects of a Pten deficiency on hepatoc autophagy, focusing our attention on each step of autophagy, i.e., t formation of autophagosomes, the maturation of autophagoson into autolysosomes, and autolysosomal degradation.

Results

Degradation of long-lived proteins under starvation conditio

To assess quantitative effects of Pten deficiency on autophagy, first examined the degradation of long-lived proteins of cultu hepatocytes. Figure 1A summarizes the data for the degradation long-lived hepatocyte proteins labeled with ^{14}C-leucine for 22 h. control hepatocytes, the degradation was markedly enhanced un starvation conditions (upper left-side box, lane A vs. upper rig side box, lane A). Under starvation conditions, the degradation w effectively inhibited in the presence of 3-methyladenine, a spec inhibitor of autophagy (lane B), E64d plus pepstatin, lysoso proteinase inhibitors (lane C), 5 mM methylamine (lane D) a 20 mM NH_4Cl (lane F) that neutralize lysosomal lumenal pH. T simultaneous addition of E64d plus pepstatin and methylamine NH_4Cl to the chase medium maximally inhibited protein degra tion (lanes E and G). In contrast, the degradation in Pten-defici hepatocytes was substantially inhibited. No large difference w found between starved and non-starved conditions and, the fracti of degradation sensitive to lysosomal proteinase inhibitors in Pt deficient hepatocytes (~3–4% under starvation conditions, lo left-side box) was much smaller than that in control hepatocy (~7–8% under starvation conditions, upper left-side box). These d clearly demonstrate that autophagic protein degradation is marke diminished in Pten-deficient hepatocytes.

The magnitude of the inhibition of autophagic protein degradati in Pten-deficient hepatocytes was comparable to that of autopha deficient hepatocytes, in which Atg7, an E1-like enzyme, which essential for autophagy, was deleted.[34] It is generally thought t the activation of Akt stimulates the mTor /P70S6-kinase pathw the activation of which causes the suppression of autophagy.[17] therefore reasoned that the inhibition of autophagy could be me ated through activation of the mTor/P70S6-kinase pathway by Pten-deficiency. We surveyed the phosphorylation state of A the ribosomal S6 subunit, and initiation factor 4E-binding prot by immunoblotting (Fig. 1B). As expected, all of these molecu

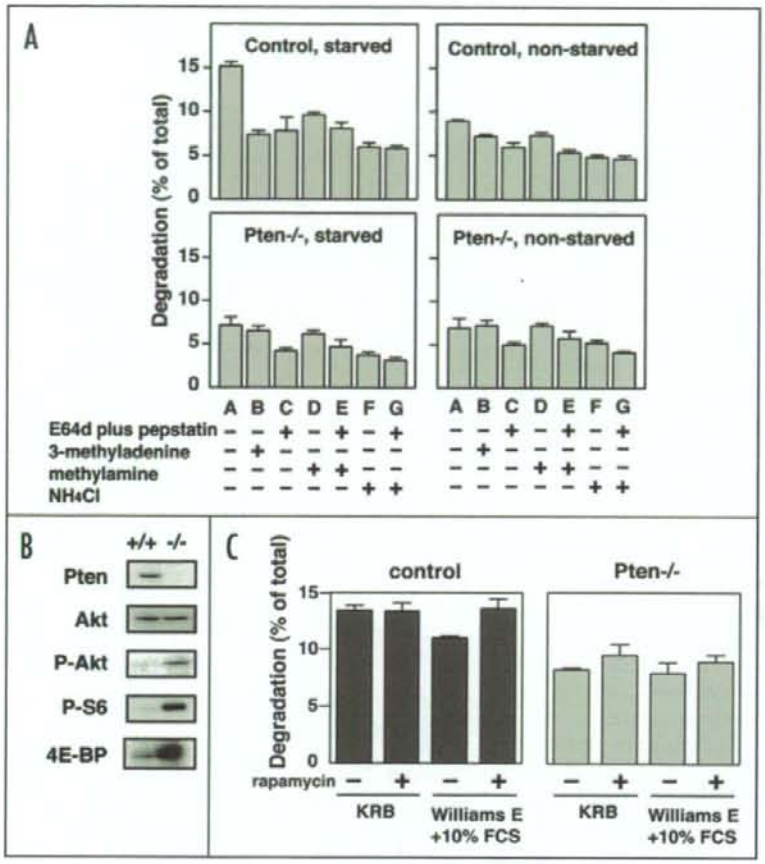

Figure 1. Degradation of long-lived proteins of control and Pten-deficient hepatocytes under starved and non-starved conditions. (A) Hepatocytes isolated from control and Pten-deficient livers were cultured in Williams E/10% FCS. The cells were then incubated with Williams E/10% FCS containing [^{14}C]-leucine (0.5 μCi/ml) for 22 h to label the long-lived proteins. The cells were then washed with Williams E/10% FCS containing 2 mM unlabelled leucine and incubated with the medium for 2 hours. The cells were washed with PBS and incubated for 4 hours with either Krebs-Ringer bicarbonate buffer (left-side boxes, starved) or Williams E/10% FCS (right-side boxes, non-starved) in the presence (lanes B to G) or absence (lane A) of various inhibitors. The inhibitors added were: 10 mM 3-methyladenine (lane B), 10 μg/ml E64d and 10 μg/ml pepstatin (lane C), 5 mM methylamine (lane D), 5 mM methylamine plus 10 μg/ml E64d and 10 μg/ml pepstatin (lane E), 20 mM NH_4Cl (lane F) and 20 mM NH_4Cl plus 10 μg/ml E64d and 10 μg/ml pepstatin (lane G). At the end of the incubation, trichloroacetic acid-soluble radioactivity released in the medium and trichloroacetic acid-insoluble radioactivity remaining in the cells were determined separately as described in Materials and Methods. Degradation (% of total) determined in triplicate assay, is expressed as the mean (%) ± S.D. (B) Whole liver lysates from control (+/+) and Pten-deficient (-/-) mice starved for 12 h were separated in SDS-polyacrylamide gels and the separated proteins were electrophoretically transferred to a PVDF membrane. Pten, Akt, phosphorylated Akt, phosphorylated ribosomal S6 and initiation factor 4E-binding protein were determined by immunoblotting analysis using respective antibodies. (C) Long-lived proteins of control and Pten-deficeint hepatocytes were labeled with [^{14}C]-leucine (0.5 μCi/ml), chased with Williams E/10% FCS containing 2 mM unlabelled leucine for 2 h, and incubated with either Krebs-Ringer bicarbonate buffer (KRB) or Williams E/10% FCS in the presence of absence of 0.2 mM rapamycin for 4 hours. Degradation (% of total) determined in triplicate is expressed as the mean (%) ± S.D.

were in the phosphorylated state in starved Pten deficient livers, while they were dephosphorylate in control livers (Fig. 1B).

We next tested whether or not rapamyci could enhance autophagic protein degradatio in Pten-deficient hepatocytes under nutrient-ric conditions. Rapamycin is known to inactivat mTor and induce autophagy even under nutrient rich conditions. When rapamycin was adde to the chase medium under both starved an non-starved conditions, rapamycin substan tially enhanced protein degradation in contr hepatocytes under non-starved conditions to level almost equivalent to that obtained unde starved conditions. In contrast, no significan enhancement was observed with Pten-deficien hepatocytes under both starved and non-starve conditions (Fig. 1C). Thus, inactivation of mTo P70S6-kinase pathway by rapamycin was nc sufficient for reversing autophagy suppression i Pten-deficient livers.

Expression of *ATG* genes in wild type an Pten-deficient livers. We next examined the possi bility that hyper-activation of Akt in Pten-deficien livers may suppress the expression of *ATG*. comprehensive DNA microarray using mRN isolated from control and Pten-deficient mous hepatocytes revealed that expression of som *ATG* genes was substantially decreased in mutan hepatocytes, compared with control hepatocyte (data not shown). This was further confirme by RT-PCR analysis (Fig. 2A). *ATG7*, *ATG3* an *ATG10* are genes that encode E1-like enzym (Atg7) and E2-like enzymes (Atg3 and Atg10 respectively, which participate in the autophagy specific protein conjugation system.[15,16] Thei expression was decreased by 20–60% in Pten deficient hepatocytes, compared with contr hepatocytes. The expression of two gene *ATG12* and *MAP-LC3*, which encode modifier (Atg12 and LC3) of the two *ATG* conjugatio systems, was also decreased to less than 50% i mutant hepatocytes, whereas expression of *ATG (BECLIN)* and *ATG16* was less affected. Thus, Pten-deficiency or hyper-activation of the class PI3-kinase/Akt pathway elicited the downregula tion of transcription of some *ATG* genes that ar essential to autophagy.

The decrease in the transcription level of thes *ATG* genes, however, did not parallel the change in protein levels of the *ATG* gene product Figure 2B shows immunoblotting analyses dat for liver homogenates. A Pten-deficiency cause hepatomegaly[23,24] and the total liver protein c mutant livers was increased by 30–50%, compare with that of control livers. Therefore, the amount of protein loaded onto SDS-polyacrylamide ge

were arranged so that the levels of *ATG* gene products per liver could be directly compared. Contrary to the data on message levels (Fig. 2A), significantly more Atg7, Atg3, Atg10 and Atg12-Atg5 conjugate were present in Pten deficient livers than in control livers (Fig. 2B). This was also the case for LC3 expression between control and mutant livers. Intriguingly, both LC3-I and LC3-II were present in Pten-deficient livers and in the control livers. LC3-I is a soluble form with a free carboxyl terminal glycine, while LC3-II is a lipidated form with its carboxyl-terminal glycine conjugated with phosphatidylethanolamine. Since it is the latter form of LC3 that is recruited onto autophagosomal membranes, the results indicate that autophagy-specific protein conjugation reactions function normally in Pten-deficient livers. In order to examine intracellular distribution of LC3-I and LC3-II, liver homogenate was separated in mitochondrial/lysosomal, microsomal and cytosolic fractions (Fig. 2C). There was no significant difference in the distribution of LC3-I and LC3-II between control and Pten-deficient livers. LC3-II was most abundant in mitochondrial/lysosomal fraction, whereas LC3-I was mainly present in the cytosolic fraction (Fig. 2C).

Morphological analysis of autophagic vacuoles in wild type and Pten-deficient livers. As LC3-II was expressed normally in mutant livers, it is important to determine whether or not autophagosomes can be formed in mutant livers under starvation conditions. The administration of leupeptin, a potent inhibitor of lysosomal cysteine proteinases, to rats and mice is known to cause the accumulation of autophagic vacuoles (autophagosomes and autolysosomes) by inhibiting lysosomal proteolysis.[35-37] We therefore injected leupeptin, as described in the Materials and Methods section, into both control and mutant mice that had been starved for 48 hours. One hour after the injection, the livers were subjected to perfusion-fixation with glutaraldehyde and examined by electron microsopy. Figure 3 shows that autophagic vacuoles were abundantly present in control livers (A and C), but only a few were observed in mutant livers (B and C). Morphometry revealed that the number of autophagic vacuoles per 100 μm^2 of hepatocyte cytoplasm in control livers is 44.37 + 13.66 (mean + S.D., n = 30) whereas that in mutant livers is 11.78 + 8.6 (mean + S.D., n = 30) (Fig. 3E). Interestingly, some vacuoles in mutant livers possessed lumenal structures with sequestered components shrunken to the center of the vacuoles (Fig. 3D, arrows). In contrast, the sequestered components in most of the vacuoles in control livers appeared to have blurred lumenal structures, suggesting that the vacuoles consist of typical autolysosomes. Thus, the accumulation of autophagic vacuoles is severely hindered in Pten-deficient livers, compared with control livers, consistent with biochemical data showing that the starvation-enhanced degradation of long-lived protein is markedly suppressed by the loss of Pten.

Assessment of autolysosomes in control and mutant livers. The decreased number of autophagic vacuoles may reflect a reduction in autophagosome formation and/or the retardation of autophagosome maturation to autolysosome. Because the levels of LC3-II, an autophgaosomal membrane marker, were slightly increased, but total number of autophagic vacuoles was markedly decreased in Pten-deficient livers, compared to control livers, we hypothesized that the autophagy dysfunction in the Pten-deficiency could be primarily attributed to an impairment in autophagosome formation. Additionally, another possibility for an impairment of autophagosome maturation into autolysosome should also be considered. In

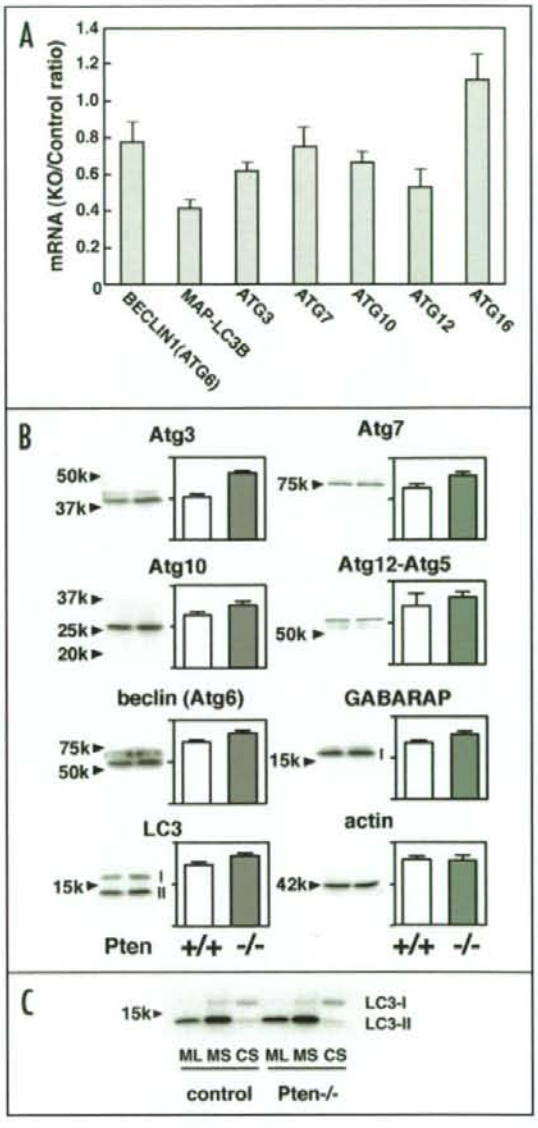

Figure 2. Expression of *ATG* gene products in control and Pten-defici livers. (A) Messenger RNAs extracted from control and Pten-deficient liv were subjected to RT-PCR analysis as described in Materials and Metho The expression levels of mRNAs were determined for some representat *ATG* genes and the ratios of the levels between Pten-deficient livers (K and control livers (Control) were plotted. (B) Immunoblotting was perform with whole cell lysates from control and Pten-deficient livers. As the total li protein of mutant livers was 1.3-fold higher than that of control livers c to hepatomegaly, 26 μg protein of mutant liver lysate and 20 μg protein control lysate were run in 10% or 12.5% SDS-polyacrylamide gels and separated polypeptides were subjected to immunoblotting analyses. D shown are representative of three separate experiments. Quantitative den tometry was performed using NIH imaging system. As for LC3, the data LC3-II are shown. (C) Mitochondrial/lysosomal (ML), microsomal (MS), c cytosol (S) fractions were isolated from normal and Pten-deficient livers described in Materials and Methods. Twenty five microgram protein of ea fraction was separated on 12.5% SDS-polyacrylamide gels and subjected immunoblotting analysis using anti-LC3 antibody.